UNIVERSITÀ
DEGLI STUDI
DI PADOVA

ICEA Department

MSc Environmental Engineering

MASTER THESIS

Marini Sara

Magnetic nanocomposites for heavy metals removal from stormwater

Supervisor: *Prof. Sgarbossa Paolo*

ACADEMIC YEAR 2014/2015

Abstract

By 2020 half the world population will probably live in urban areas, causing the increase in the volume of stormwater needing treatment. Heavy metals are the most common pollutants in urban dust and runoff. Many techniques have been developed to remove heavy metals from wastewater both in the past (conventional techniques) and in recent years (alternative techniques). All these methods present different drawbacks and problems, therefore new methods of treatment must be developed in the near future. Iron oxide nanocomposites may be an efficient tool to solve this problem. The present thesis studies new iron oxide/graphene oxide nanocomposites, evaluating their morphologic and magnetic properties and assessing their performance in removing lead, chromium and nickel. These nanocomposites can efficiently be removed, after their application, simply by applying a magnet as demonstrated by the results obtained through magnetic measurements and magnetic separation after adsorption experiments. The removal efficiencies obtained depends on the heavy metal treated. Among the heavy metals analyzed, the removal was more efficient for lead than for chromium and nickel.

Metà della popolazione mondiale abiterà probabilmente nelle aree urbane entro il 2020, causando l'aumento dei volumi di acqua di prima pioggia da trattare. I metalli pesanti sono gli inquinanti più comuni nelle acque meteoriche di dilavamento. In passato e negli ultimi anni sono state sviluppate diverse tecniche per la rimozione dei metalli pesanti dalle acque reflue. Questi metodi di trattamento presentano diversi svantaggi e problemi, perciò nuovi metodi di trattamento dovranno essere sviluppati nel prossimo futuro. I nanocompositi di ossidi di ferro possono essere un efficiente strumento per risolvere questo problema. La presente tesi studia nuovi nanocompositi, esaminando le loro caratteristiche morfologiche e magnetiche e valutando la loro performance nella rimozione del piombo, del cromo e del nickel. Dopo l'applicazione, questi nanocompositi possono essere rimossi semplicemente tramite separazione magnetica, come dimostrato dai risultati ottenuti tramite misurazioni magnetiche e dalle prove sperimentali di separazione magnetica successive agli esperimenti di adsorbimento. Le efficienze di rimozione ottenute variano in base al metallo considerato. La rimozione è più elevata nel caso del piombo rispetto al cromo e al nichel.

Index

1. Stormwater pollutants and legislation

Pollution generated by urban run-off is an important environmental problem especially for the extremely varied nature of the type of pollutants, which depends mainly on the nature of the anthropogenic activities occurring in the interested area. The pollutants include organic compounds (such as polycyclic aromatic hydrocarbons (PAHs), polychlorinated biphenyls (PCBs), atrazine), nutrients and heavy metals (such as lead, mercury, chromium) which are widely spread and difficult to remove. Table 1.1 shows common stormwater pollutants and their sources.

Table 1.1: Pollutants and their sources in stormwater runoff [1].

	Soil erosions	Vehicles	Human/animal waste	Fertilizers	Household chemicals	Industrial processes	Paint and preservatives
Solids	■	■	■				
Metals	■	■					
Oil, greese and organics		■			■	■	■
Nutrients	■		■	■	■	■	

By 2020 half the world population will probably live in urban areas causing the increase in the volume of stormwater needing treatment [1].

Heavy metals are the most common pollutants in urban dust and runoff. They are particularly dangerous because of their high solubility in water, which means they can easily enter and spread in the environment, and consequently enter the food chain [2]. There are many different definitions for heavy metals, based on density, on atomic weight or on their chemical properties and their toxicity. In urban environments, heavy metals usually refer to toxic metals that originate from human activities [1].

Excess levels of these heavy metals can damage human health and ecosystems. However some of these same elements are required in trace amounts by human and living organisms. The heavy metals of most concern in the environment are chromium (Cr), nickel (Ni), zinc (Zn), copper (Cu), lead (Pb), vanadium (V), cobalt (Co), cadmium (Cd) and mercury (Hg).

Heavy metals cause important harmful health effects, such as reduced growth and development, cancer, organ damage, nervous system damage, and death. Moreover, some metals, such as mercury and lead, may cause development of autoimmunity (a person's immune system attacks the harmless cells of its own body) [2].
The type and amount of heavy metals present in stormwater depends on many factors such as:

- land use characteristics;
- specific materials and components employed in the drainage area;
- meteorological effects.

In non-industrial areas the main sources of heavy metals are automobiles and structures with metallic components [3].
Davis et al. [3] reported the major source for each heavy metal, such as the brakes for copper, the tire wear for zinc and the vehicles' surfaces for chromium, since they are coated with hexavalent chromium to prevent corrosion.
Table 1.2 presents several heavy metals concentration range in the sediments on street surfaces as a function of sediment grain size. Sediments were collected in an area close to London. The concentration is higher in the case of coarse sediments.

Table 1.2: Heavy metals range as a function of sediment grain size [1].

	Sediment size < 250 µm	**Sediment size > 250 µm**
Pb (µg/g)	40-1690	111-2296
Cd (µg/g)	0,72-4,2	1,3-6,8
Mn (µg/g)	766-855	694-1244
Zn (µg/g)	119-2133	91,6-1760
Cu (µg/g)	42,6-640	27,2-212
Fe (µg/g)	6780-22700	4195-22850

Due to their toxicity and harmfulness, heavy metals discharge to the environment has been regulated by laws throughout the world. The limit concentration established by law for water discharge varies with the type of heavy metal and from country to country.
In Italy this limit concentrations are established by Legislative Decree 152/2006 (Table 1.3).

Table 1.3: Limit concentration for water discharge according to legislative decree 152/2006 [4].

Parameters	**Unit of measure**	**Discharge in surface waters**	**Discharge in sewer system**
pH		5,5-9,5	5,5-9,5
BOD_5 (as O_2)	mg/l	≤ 40	≤ 250
COD (as O_2)	mg/l	≤ 160	≤ 500
Alluminum	mg/l	≤ 1	≤ 2,0
Arsenic	mg/l	≤ 0.5	≤ 0.5
Barium	mg/l	≤ 20	-
Boron	mg/l	≤ 2	≤ 4
Cadmium	mg/l	≤ 0,02	≤ 0,02
Total chromium	mg/l	≤ 2	≤ 4
Chromium (VI)	mg/l	≤ 0,2	≤ 0,20
Iron	mg/l	≤ 2	≤ 4
Manganese	mg/l	≤ 2	≤ 4
Mercury	mg/l	≤ 0.005	≤ 0.005
Nickel	mg/l	≤ 2	≤ 4
Lead	mg/l	≤ 0,2	≤ 0,3
Copper	mg/l	≤ 0,1	≤ 4
Selenium	mg/l	≤ 0,03	≤ 0,03
Tin	mg/l	≤ 10	-
Zinc	mg/l	≤ 0,5	≤ 1,0
Total cyanide	mg/l	≤ 0,5	≤ 1,0
Free available chlorine	mg/l	≤ 0,2	≤ 0,3
Sulfide (as H_2S)	mg/l	≤ 1	≤ 2
Sulfite (as SO_3)	mg/l	≤ 1	≤ 2
Sulfate (as SO_4)	mg/l	≤ 1000	≤ 1000
Chloride	mg/l	≤ 1200	≤ 1200
Fluoride	mg/l	≤ 6	≤ 12
Total phosphorus (as P)	mg/l	≤ 10	≤ 10
Ammoniacal nitrogen (as NH_4)	mg/l	≤ 15	≤ 30
Nitrous nitrogen (as N)	mg/l	≤ 0,6	≤ 0,6
Nitric nitrogen (as N)	mg/l	≤ 20	≤ 30
Fats and oils	mg/l	≤ 20	≤ 40
Total hydrocarbons	mg/l	≤ 5	≤ 10
Phenols	mg/l	≤ 0,5	≤ 1
Aldehydes	mg/l	≤ 1	≤ 2
Aromatic organic solvents	mg/l	≤ 0,2	≤ 0,4
Nitrogen organic solvents	mg/l	≤ 0,1	≤ 0,2
Total surfactants	mg/l	≤ 2	≤ 4
Total pesticides	mg/l	≤ 0,05	≤ 0,05
Chlorinated solvents	mg/l	≤ 1	≤ 2

With regard to stormwater, the Legislative Decree 152/2006 establishes that regions are responsible for deciding when and which amount of stormwater needs to be treated in a wastewater treatment plant. For example Lombardia's legislation defines stormwater as the first 5 mm/m^2 of rainwater, due to their relatively high concentration of pollutants [5]. Whenever these waters come from industrial soil, parking, oil stations etc., they must be conveyed and treated in sewage treatment plants.

Heavy metals limits for discharge in sewer system are compulsory in absence of specific limits defined by the competent (regional) authority, or whenever the final treatment plant cannot assure that final limit concentrations for discharge in surface waters can be reached. Also whenever stormwater coming from parking, oil stations etc., is discharged directly on soil, heavy metals removal may be necessary. In this last case, heavy metals concentration limits before discharge are those presented in Table 1.4.

Table 1.4: Limits for discharge on soil.

Parameters	**Unit of measure**	**Discharge on soil**
pH		6-8
BOD_5 (as O_2)	mg/l	≤ 20
COD (as O_2)	mg/l	≤ 100
Total nitrogen (as N)	mg_N/l	≤ 15
Total phosphorus (as P)	mg_P/l	≤ 2
Total surfactants	mg/l	≤ 0,5
Alluminum	mg/l	≤ 1
Arsenic	mg/l	≤ 0,05
Barium	mg/l	≤ 10
Boron	mg/l	≤ 0,5
Total chromium	mg/l	≤ 1
Iron	mg/l	≤ 2
Manganese	mg/l	≤ 0,2
Nickel	mg/l	≤ 0,2
Lead	mg/l	≤ 0,1
Copper	mg/l	≤ 0,1
Selenium	mg/l	≤ 0,002
Tin	mg/l	≤ 3
Zinc	mg/l	≤ 0,5
Free available chlorine	mg/l	≤ 0,2
Sulfide (as H_2S)	mg/l	≤ 0,5
Sulfite (as SO_3)	mg/l	≤ 0,5
Sulfate (as SO_4)	mg/l	≤ 500
Chloride	mg_{Cl}/l	≤ 200
Fluoride	mg_F/l	≤ 1
Phenols	mg/l	≤ 0,1
Aldehydes	mg/l	≤ 0,5
Aromatic organic solvents	mg/l	≤ 0,01
Nitrogen organic solvents	mg/l	≤ 0,01

2. Heavy metals removal from water

Many techniques are available to treat heavy metals, however some criteria are important to choose the best one:

- Applicability to local condition.
- Ability to reach the legal limit concentration as defined by law.

Innovative processes for treating wastewater containing heavy metals are the most widely studied and applied. However, lime precipitation, a conventional method of treatment, is one of the most efficient techniques to treat inorganic effluents with a metal concentration higher than 1000 mg/l. The present paragraph reviews the different methods, both conventional and innovative ones.

2.1 Conventional methods

Conventional methods to treat metal contaminated water are [2]:

- Chemical precipitation.
- Ion exchange.
- Electrochemical removal.

2.1.1 Chemical precipitation

The method of chemical precipitation can be summarized by the following precipitation equation (M^{2+} are the dissolved metal ions, OH^- represents the precipitant and $M(OH)_2$ is the insoluble metal hydroxide).

$$M^{2+} + 2OH^- \leftrightarrow M(OH)_2 \downarrow$$

The major parameter affecting this method is the pH, which needs to be adjusted to basic conditions. The most common precipitant agents used are lime and limestone (composed of calcium carbonate, $CaCO_3$). Lime precipitation is efficient to treat inorganic effluents with concentrations higher than 1000 mg/l. Although the technique

is cheap, safe and simple, it requires the use of a large amount of chemicals in order to reduce metal content to an acceptable level before discharge. Furthermore, it creates a lot of sludge needing treatment. Other minor drawbacks are slow metal precipitation, poor settling, aggregation of metal precipitates, long-term environmental impacts of sludge disposal.

2.1.2 Ion exchange

Ion exchange. Ion exchangers are capable of exchanging ions with the surrounding material. The most common are synthetic, organic resins, which generally can be regenerated on site by treatment with acid or caustic soda. This method has many drawbacks, the most important being that it cannot treat water with high metal concentration, because of fouling of the matrix by organics and other solids present in the wastewater. Furthermore, ion exchange is nonselective and highly sensitive to pH.

2.1.3 Electrochemical removal

This technique is based on the passage of a current by a cathode plate and an insoluble anode through the water stream. Metal cations present in water are attracted by the negatively charged cathode and stick to it. A metal deposit forms on the cathode and can be removed. The main drawback is that electrodes may be easily corroded, so they may have to be replaced frequently.

2.2 Alternative techniques

As shown there are many disadvantages in applying conventional techniques, such as large chemical requirements, production of high amounts of sludge and fouling. Although these methods can still be useful in some cases, new techniques can treat water in a more efficient way, by minimizing drawbacks. The most important alternative techniques are:

- Adsorption.
- Membrane filtration.

- Electrodialysis.
- Photocatalysis.

2.2.1 Adsorption

The most important alternative technique is adsorption, a mass transfer process. Adsorption consists in the transfer of a substance from the liquid phase to the surface of a solid. The substance may be bound by physical and/or chemical interactions. The process is composed of three main steps [2]:

1. Transport of the pollutant from the bulk solution to the sorbent surface.
2. Adsorption on the solid surface.
3. Transport within the sorbent particle.

Currently, the most popular method for the removal of heavy metals from water is immobilization through adsorption on activated carbon, a cheap and easy to apply technique. Many other adsorbents have been studied; these may have mineral, organic or biologic origin [2]:

- Zeolites (aluminosilicate minerals composed of aluminum, silicon and oxygen). Clinoptilolite, the most important natural zeolite, showed high selectivity for some particular heavy metal ions, e.g. Pb(II), Cd(II), Zn(II), and Cu(II). However its efficiency is highly dependent on the pretreatment. Instead, synthetic zeolite selective adsorption is highly pH dependent.

- Clay-polymer composites are natural clay minerals (hydrous aluminum phyllosilicates) modified with a polymeric material in order to improve the polymer efficiency in removing metals.

- Phosphates, such as calcined phosphate, activated phosphate (with nitric acid), and zirconium phosphate.

- Industrial byproducts, for example fly ash, iron slags, hydrous titanium oxide. All these material can be chemically modified in order to remove heavy metals from water.

- Modified agricultural and biological wastes. In this case the process is called bio-sorption and utilizes inactive (non-living) microbial biomass to bind heavy metals by purely physico-chemical mechanisms (mainly chelation and adsorption). Some examples are hazelnut shell, rice husk, pecan shells, jackfruit, maize cob or husk. These need to undergo chemical modification or conversion by heating into activated carbon before use.

- Biopolimers. These have a lot of positive features, such as capability of lowering transition metals ion concentration to an order of magnitude lower than parts per billion; availability; environmental safety. Moreover their different functional groups (hydroxyls, amines, etc.) increase the efficiency of metal ion uptake and the maximum chemical loading possible.

- Hydrogels, crosslinked hydrophilic polymers. Removal is driven by water diffusion into the hydrogel. Hydrogels expand their volume thanks to their high swelling in water.

2.2.2 Membrane filtration

Membrane filtration is another method whose use is constantly increasing in the last years. It allows to remove a wide range of contaminants: suspended solids, organic and inorganic compounds (e.g. heavy metals). There are three types of membrane filtration: ultrafiltration (UF), nanofiltration (NF) and reverse osmosis (RO). This classification is based on the size of the particles that can be retained by the membrane: UF > NF > RO. Therefore generally NF membranes separation efficiency is between the UF and RO ones. The three types of filtration combined can be used to obtain multiple barriers in order to increase the efficiency.

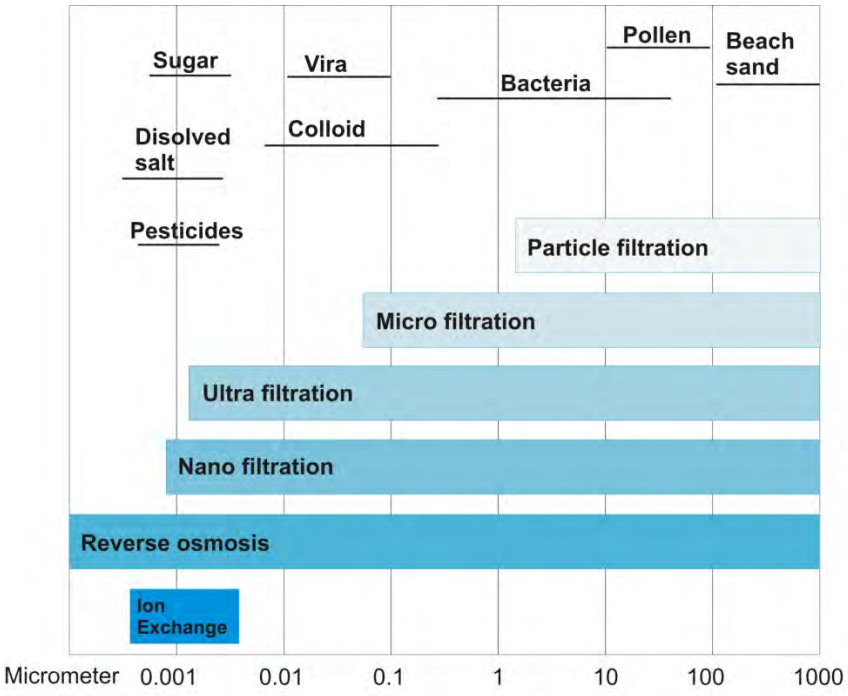

Figure 2.1: Comparison between the different types of filtration [6].

In ultrafiltration (UF) a permeable membrane separates macromolecules, suspended solids and heavy metals from water. The pore size ranges from 5 to 20 nm and the molecular weight of the separating compounds from 1000 to 100000 Da. With a metal concentration ranging from 10 to 112 mg/l, UF can reach a removal efficiency higher than 90%. However, fouling has many adverse effects on the membrane (e.g. flux decline, increase in transmembrane pressure), which result in high operational costs [2].
Reverse osmosis is sometimes used to remove low levels of heavy metals from drinking water. However this method is costly and easily subject to clogging (the same metal oxides tend to clog the membrane).

2.2.3 Electrodialysis

Electrodialysis (ED) is a particular membrane separation process. Water pass through ion exchange membranes composed of thin sheets of plastic materials with either anionic or cationic characteristics and an electric potential is applied. The anions present in solution migrate toward the anode and the cations toward the cathode, crossing the ion exchange membranes ([7], Figure 2.2).
ED produces a highly concentrated stream and allows to recover valuable metals such as Cr and Cu. Like the other membrane techniques, ED requires periodic maintenance.

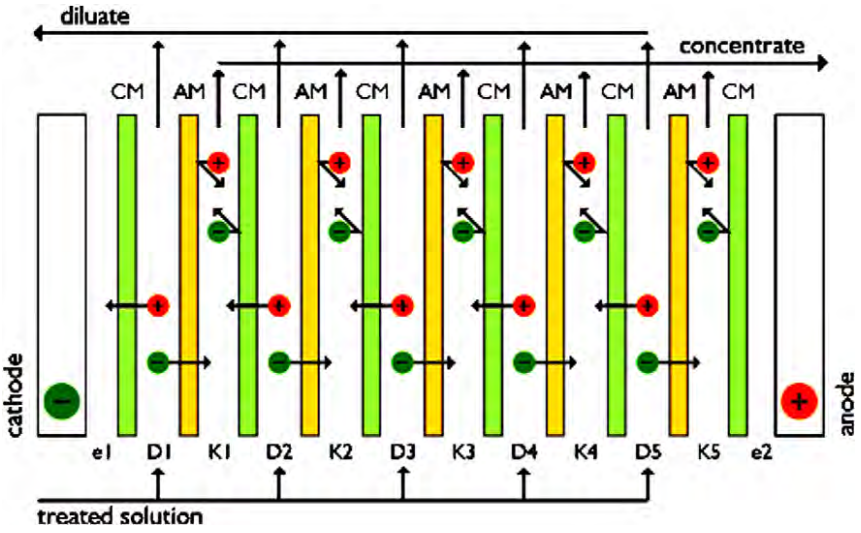

Figure 2.2: Electrodialysis scheme. CM, cation-exchange membrane, D, diluate chamber, e1 and e2 – electrode chambers, AM, anion exchange membrane, and K, concentrate chamber [7].

2.2.4 Photocatalysis

Photocatalysis in an alternative process that utilizes solar energy. The classical photocatalysis is composed of five steps [8]:

1. Transfer of the reactants in the fluid phase to the surface of the catalyst.
2. Adsorption the reactants.
3. Reaction in the adsorbed phase.
4. Desorption of the products.
5. Removal of the products from the interface region

The photocatalytic reaction occurs during step n° 3, in the adsorbed phase. When the semiconductor–electrolyte interface is hit by light with energy equal or greater than the semiconductor band-gap, electron–hole pairs (e-/h+) form and dissociate into free photo-electrons in the conduction band and photoholes in the valence band.

At the same time, if a fluid phase (gas or liquid) is present, a spontaneous adsorption occurs and electrons are transferred towards acceptor molecules, whereas positive photoholes are transferred to donor molecules (according to the redox potential of each adsorbate) [8]. That is to say, the charge carriers migrate toward the semiconductor surface and are capable of reducing or oxidizing species in solution (Figure 2.3, [2]).

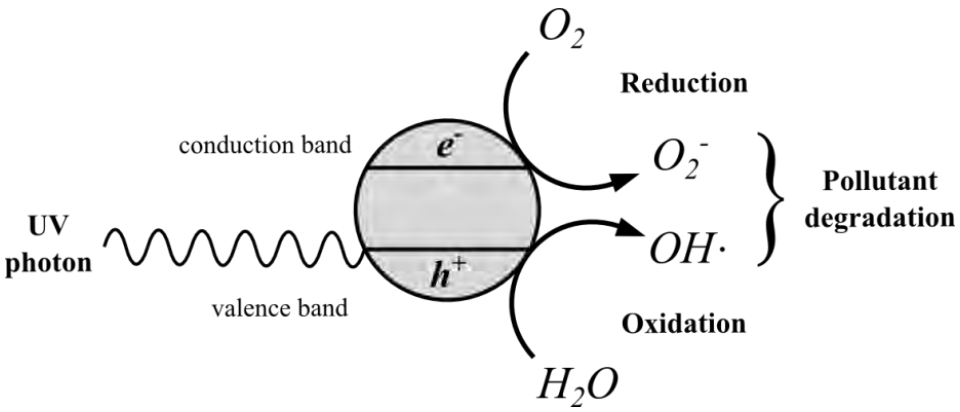

Figure 2.3: Scheme of photocatalysis over TiO_2.

All these alternative techniques have many benefits but also a lot of important drawbacks, which can be summarized in (Table 2.1, [2]):

- High operational costs due to the chemicals used.
- High-energy consumption.
- Handling costs for sludge disposal.

Table 2.1: Advantages and drawbacks of the main techniques for heavy metal treatment in wastewater.

Treatment method	Advantages	Disadvantages	References
Chemical precipitation	Low capital cost, simple operation	Sludge generation, extra operational cost for sludge disposal	Kurniawan et al. (2006)
Adsorption with new adsorbents	Low-cost, easy operating conditions, having wide pH range, high metal binding capacities	Low selectivity, production of waste products	Babel and Kurniawan (2003); Aklil et al. (2004)
Membrane filtration	Small space requirement, low pressure, high separation selectivity	High operational cost due to membrane fouling	Kurniawan et al. (2006)
Electrodialysis	High separation selectivity	High operational cost due to membrane fouling and energy consumption	Mohammadi et al. (2005)
Photocatalysis	Removal of metals and organic pollutant simultaneously, less harmful by-products	Long duration time, limited applications	Barakat et al. (2004); Kajitvichyanukula et al. (2005)

Considering the relevant drawbacks of both conventional and alternative techniques, it is still necessary to develop more efficient techniques for stormwater pollutants

treatment. In recent years, the environmental remediation research studies have been focused on the design and development of nanosized materials for adsorption of organic and heavy metal pollutants [9].

To tackle the problem of stormwater treatment, the present thesis analyzes the use of magnetically separable nanocomposites. These composites may allow to reduce the sludge produced and to improve the quality of the treated effluent.

3. Safe and sustainable water treatment with magnetic nanoparticles

Nanomaterials and nanostructures have at least one dimension in the order of magnitude of nanometers (between 1 and 100 nm) [10]. Typically a nanoparticle consists of 10 - 10^5 atoms and is smaller than a bacterial cell, whose diameter is about 1 µm (1000 nm) [11, 12].

Many of these nanomaterials, such as metal and metal oxide nanoparticles have a higher reactivity if compared to the corresponding bulk material thanks to their higher surface area/volume ratio. The peculiar reactivity may be caused by the increasing number of surface atoms with decreasing particle size. In other words, particle surface area increases with decreasing particle size, as shown in Figure 3.1. For this reason they present also different optical, electrical and magnetic properties with respect to microscopic particles [10].

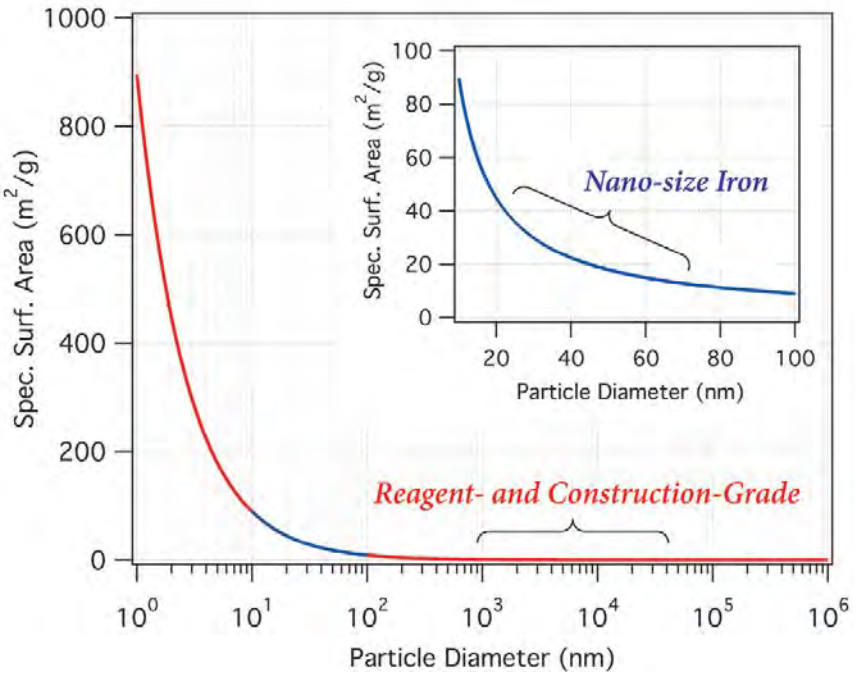

Figure 3.1: Particle surface area varying with diameter. (Surface area was calculated assuming spherical geometry and the average density of Fe^0 and Fe_3O_4, 6,7 g/cm^3) [13].

Nowadays magnetic nanoparticles, particularly nano zero-valent iron (nZVI), magnetite (Fe_3O_4) and maghemite (γ-Fe_2O_3) nanoparticles, and their applications in water

treatment are an important field of research. They show have a capacity for metals uptake from water thanks to some peculiar properties:

- High surface to volume ratio, as explained above, which implies fast kinetics for contaminant removal [14].

- Magnetism, a very useful property and, compared to sophisticated membrane filtration, a more cost effective method to separate nanoparticles from water, even though no successful real application has been reported yet [15]. This property will be explained more in detail in the following paragraph.

- Ability for surface modification, by covering the particles with inorganic shells or by attaching organic molecules to them. These properties may be used to stabilize the particles in order to prevent their oxidation but also to provide them with specific functionalities, for example, to make them selective in ion uptake [1].

- Low toxicity. Iron is a micronutrient, a substance essential for grow and survival in low amounts. However it can have adverse effects on living organisms at high concentrations.

- Low price. Considering these nanoparticles can be synthetized using mainly iron salts, their price is limited, especially if compared with that of other types of nanomaterials, for example gold nanoparticles.

Iron oxide is naturally abundant in nature in the forms of magnetite, Fe_3O_4 and maghemite, γ-Fe_2O_3. Hematite shows weak, size-dependent magnetism while maghemite shows strong ferromagnetism [16].
The magnetic nanoparticles performance in removing contaminants depends on the removal mechanisms applied. The mechanism of heavy metals removal by magnetic nanoparticles can proceed through different processes such as (Figure 3.2):

- Adsorption
- Reduction
- Co-precipitation

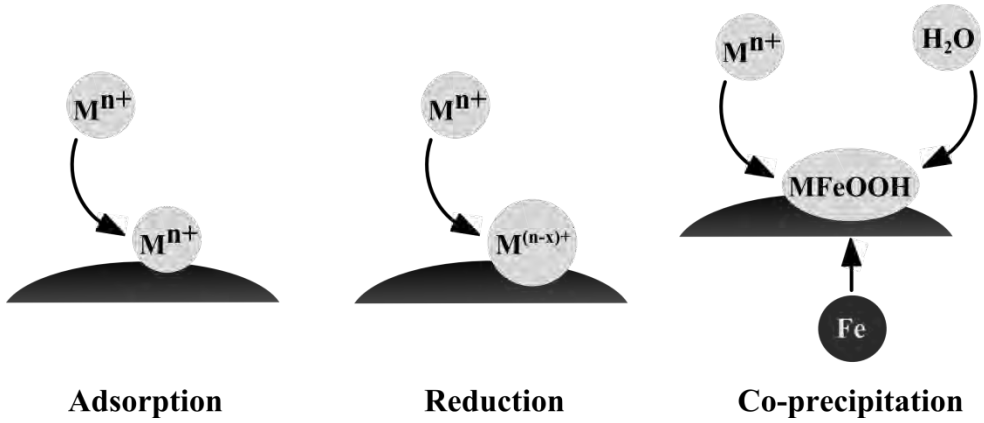

Figure 3.2: Different removal mechanisms used by magnetic nanoparticles.

Magnetite nanoparticles remove heavy metals by both physical and chemical adsorption, while maghemite particles usually gives only physical adsorption. This is demonstrated also by the low desorption of metals at high pH that occurs when applying magnetite, Fe_3O_4, nanoparticles, typical of chemical adsorption. Instead adsorption by γ-Fe_2O_3 nanoparticles does not involve chemical reaction as demonstrated by the unchanged crystallite structure after metals removal. As a matter of fact elettrostatic interactions are the cause of pollutant removal by maghemite nanoparticles.

Removal performance of magnetite and maghemite nanoparticles is highly pH dependent. At pH values below the zero point of charge (pH_{zpc}), also called isoelectric point (IEP), the surface of iron oxide nanoparticles is positively charged and therefore attracts negatively charged pollutants such as Cr (IV) and As (V) [15].

3.1 Magnetic behaviour

The movements of particles that have both mass and electric charges (e.g. electrons, holes, protons, and positive and negative ions) are the cause of magnetic effects. A magnetic dipole, so-called magneton, is composed of a spinning electric-charged particle. A magnetic domain or Weiss domain in a ferromagnetic material is a volume in which all magnetons are aligned in the same direction [17]. This domain structure is the reason why the magnetic behavior of ferromagnetic material is size dependent. As a matter of fact, iron oxide nanoparticles, unlike zero valent iron particles, show super-paramagnetic properties [14]. Superparmagnetic properties are caused by nanoparticles'

size and can be explained analyzing the coercivity, the main parameter describing the ferromagnetic material reaction to a magnetic field.

There are two different notions of coercivity, one defined in the M(H) graph and the other in the B(H) graph. In both cases the coercivity is represented by the point of intersection of the function with the negative H axis (Figure 3.3, [18]). M is the magnetization inside the sample induced by the applied magnetic field, H. B is defined as $B=\mu_0(H+M)$. The coercivity analyzed in this thesis is the intrinsic coercivity. In the following paragraphs it will be called simply coercivity.

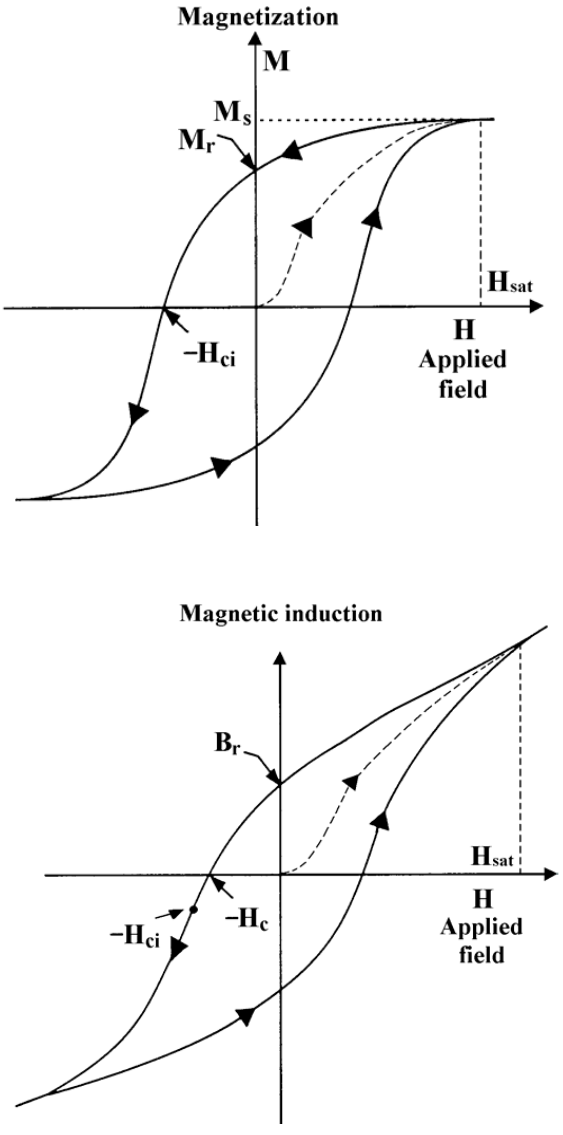

Figure 3.3: M vs H, hysteresis curve for a ferromagnetic material. M_s is the saturation magnetization. M_r, M at H equal to zero, is the residual magnetization. H_{ci} is the intrinsic coercivity, i.e. the field that reduces M to zero. $B=\mu_0(H+M)$ vs H, another hysteresis curve for ferromagnetic materials. B_r is the residual induction when H=0. H_c is the coercivity, the field that reduces B to zero [18].

When the nanoparticle diameter decreases, the coercivity increases to a maximum and then decreases toward zero. If the diameter of a single domain particle further decreases, the coercivity becomes zero and the particle is superparamagnetic (Figure 3.4).

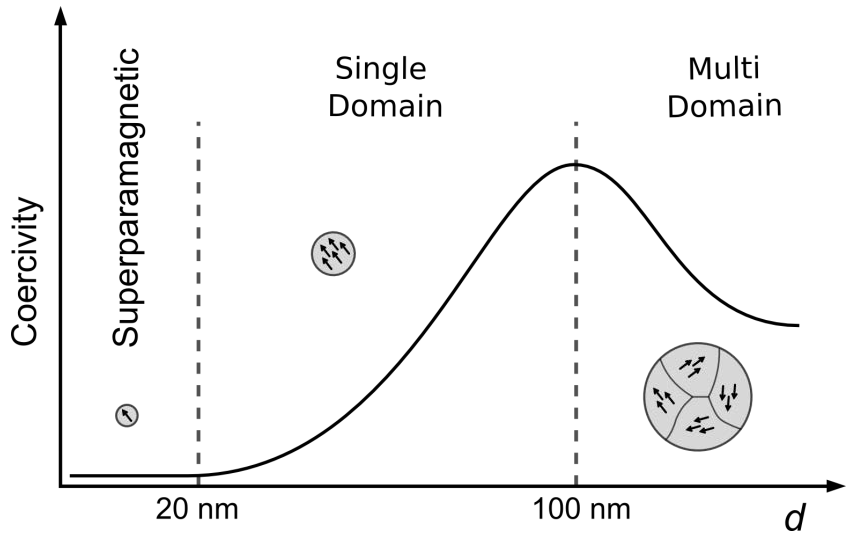

Figure 3.4: Coercivity variation with particle diameter.

Superparamagnetic nanoparticles exhibit a magnetic behavior in the presence of an external magnetic field but get back to a nonmagnetic state when the external magnet is removed while ferromagnetic nanoparticles maintain a net magnetization also after the magnet removal (Figure 3.5). Between the naturally occurring minerals on earth (e.g. Fe, Co, Ni crystalline materials show ferromagnetic properties), magnetite, Fe_3O_4, is the most magnetic [17].

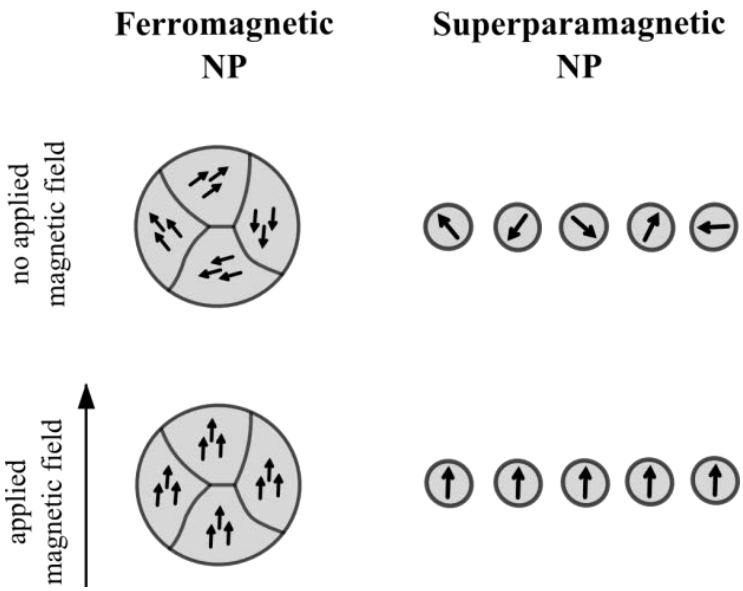

Figure 3.5: The domains of a ferromagnetic NP and the magnetic moment of single domain superparamagnetic NPs align with the applied magnetic field. However if the external magnet is removed, while ferromagnetic nanoparticles maintain their magnetization, superparamagnetic nanoparticles will show no net magnetization.

There are two main advantages of superparamagnetic nanoparticles:

- Higher reactivity thanks to the higher surface to volume ratio, as explained previously.
- Greater tendency to mix in solution, thanks to the absence of a net magnetization when no magnet is applied.

4. Magnetic iron oxide nanoparticles synthesis and functionalizations

There are two main challenges that must be overcome when synthetizing superparamagnetic nanoparticles:

1. Define experimental conditions that allow to obtain nanoparticles with suitable size. Moreover, the size dispersion must be low, to assure that all particles are at the nanoscale and present the same properties.
2. Select a process that is easily reproducible by industries.

Many methods were developed to synthesize magnetic iron oxide nanoparticles [19]:

- Coprecipitation.
- Reactions in constrained environment.
- Hydrothermal and high-temperature reactions.
- Sol-gel reactions.
- Polyol methods.
- Flow injection synthesis.
- Electrochemical methods.
- Aerosol/Vapor methods.
- Sonolysis.

Coprecipitation, the most common, efficient and easiest method. Two stages are involved in this process: a short burst of nucleation, when the reactants concentrations reaches critical supersaturation and a slow growth of the nuclei, by diffusion of the solids to the surface of the crystals. Iron oxides (Fe_3O_4 or γFe_2O_3) are prepared by mixing ferrous and ferric salts in aqueous medium. Since particles number is defined during the first step, also size control must be generally performed in this stage of the process. The reaction representing Fe_3O_4 formation is:

$$Fe^{2+} + 2Fe^{3+} + 8OH^- \rightarrow Fe_3O_4 + 4H_2O$$

Complete precipitation of Fe_3O_4 is expected at a pH ranging from 8 to 14, with a stoichiometric ratio Fe^{3+}/Fe^{2+} of 2:1 in a non-oxidizing oxygen environment (since the oxygen used to oxidize iron is the one present in OH^- ions, therefore the oxygen is already reduced). Moreover the higher the pH and the closer the stoichiometric ratio Fe^{3+}/Fe^{2+} to 2:1, the smaller the particles size and the size distribution with will be. Also increasing the mixing rate allows to reduce particles size.
Since magnetite, Fe_3O_4, is not stable, it is transformed into maghemite γFe_2O_3 in the presence of oxygen:

$$Fe_3O_4 + 2H^+ \rightarrow \gamma Fe_2O_3 + Fe^{2+} + H_2O$$

Reactions in constrained environment, as many other methods, was developed to produce nanoparticles with more uniform dimensions with respect to those obtained with the coprecipitation method. This technique utilizes synthetic and biological nanoreactors. Surfactant molecules may spontaneously form nanodroplets of different sizes:

- micelles (1-10 nm)
- water-in-oil emulsions (10-100 nm)

In these nanodroplets aqueous iron salt solutions are encapsulated by a surfactant coating that separates them from a surrounding organic solution. Consequently, this system forms a nanoreactor since it applies kinetic and thermodynamic constraints on particle formation. These constraints limit particle nucleation and growth.

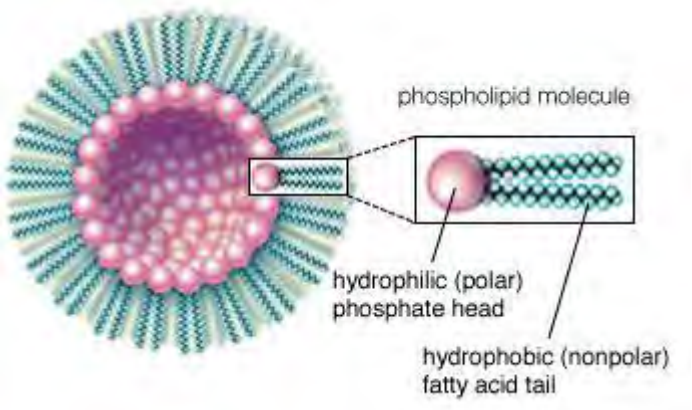

Figure 4.1: Reverse micelle structure.

Hydrothermal and high-temperature reactions. These processes are carried out in acqueous media in reactors or autoclaves characterized by very high temperatures and pressures (pressure can be higher than 2000 psi, temperature higher than 200°C). There are two similar and alternative routes to obtain iron oxide nanoparticles with this method: hydrolysis and oxidation or neutralization of mixed metal hydroxides. The main difference between these two routes is that the first one utilizes iron salts. In both cases, as it often occurs in nanoparticles synthesis, reaction conditions significantly affected the product characteristics. For example, a prolonged reaction time and higher water content increased the size of the nanoparticles obtained.

Sol-gel reactions, based on the hydroxylation and condensation of molecular precursors in solution, forming a "sol" of nanometric particles. The wet gel, a three dimensional metal oxide network, was obtained by further condensation and inorganic polymerization. Since these reactions occur at room temperature, a final heat treatment is needed to reach the final crystalline state.

Polyol methods, similar to sol-gel reactions. Polyols used ad solvents have some interesting characteristics. They can dissolve inorganic inorganic compounds thanks to their high dielectric constants. They can be used to prepare inorganic compounds in a wide operating-temperature range because of their high boiling points. Furthermore, polyols avoid interparticle aggregation.

Flow injection synthesis, used to obtain particles with narrow size distribution and to define the particle morphology. The reaction zone is confined in different "matrixes" such as emulsions. An alternative to the "matrix" confinement can be a specific design of the reactor. The obtained particles have a narrow sized distribution ranging from 2 to 7 nm.

Electrochemical methods. Preparation of iron oxide nanoparticles from an iron electrode in an aqueous solution of dimethylformamide and cationic surfactants.

Aerosol/Vapor methods. Spray and laser pyrolysis have the main advantage to be continuous chemical processes allowing high rate production. In spray pyrolysis after a solution of ferric salts and a reducing agent in organic solvents is sprayed into a series

of reactors, the aerosol solute condenses and the solvent evaporates. Particles size in the resulting dried residue depends on the initial size of the original droplets. Laser pyrolysis allows to reduce the reaction volume. Small, narrow sized nanoparticles are produced by laser heating a gaseous mixture of iron precursor.

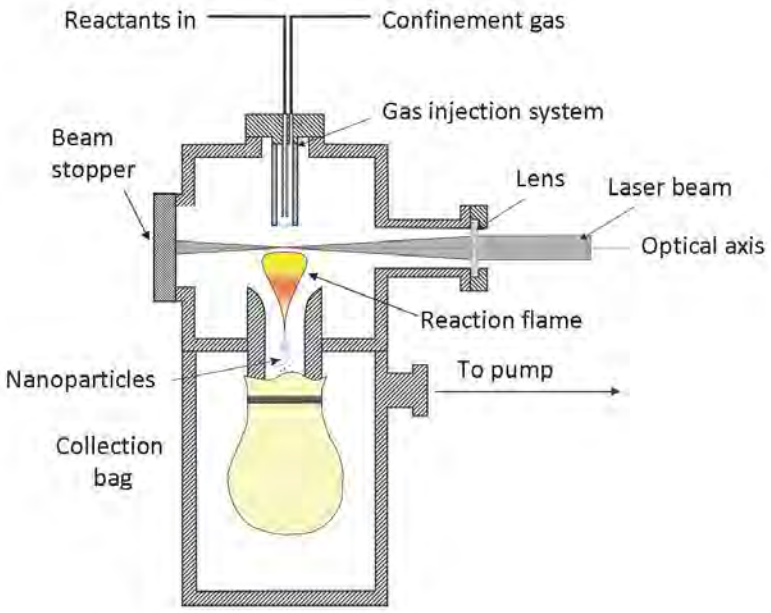

Figure 4.2: Scheme of laser pyrolysis [20].

Sonolysis, breaking of chemical bonds or radicals formation by using ultrasound, Figure 4.3. The rapid collapse of sonically generated cavities originates very high temperature hot spots allowing for the conversion of ferrous salts into magnetic nanoparticles.

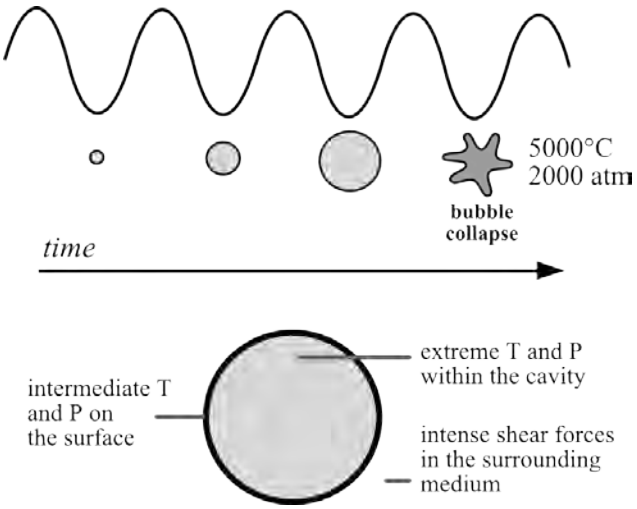

Figure 4.3: Sonolysis process. Applying ultrasound, alternate compression and rarefaction of the liquid causes pressure drops leading to the formation of small gas bubbles. The bubbles collapse after reaching an unstable size.

4.1 Stabilization of magnetic particles

Iron oxide nanoparticles must be stabilized against aggregation by reaching the equilibrium between attractive and repulsive forces in the magnetic colloidal suspension.
There are four types of forces that theoretically contribute to the interparticle potential in the system:

1. Van der Waals forces that induce strong short range isotropic attractions.
2. Electrostatic repulsive forces that can be partially screened adding salt to the suspension.
3. Magnetic dipolar forces between two particles, in case of magnetic suspensions.
4. Steric repulsion forces, in case of non-naked particles.

The first three types of forces are globally attractive as can be demonstrated integrating the anisotropic interparticle potential over all directions. Stabilization of the particles can be achieved acting on one or both of the two repulsive forces (electrostatic and steric repulsion, Figure 4.4).

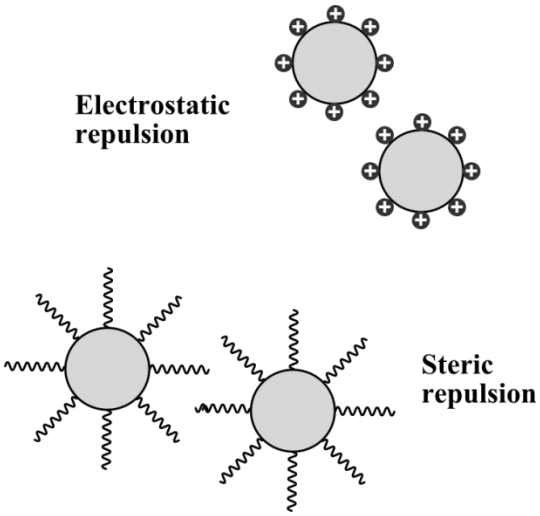

Figure 4.4: Particles are stabilized by an electrostatic layer or by steric repulsion.

The surface iron atoms of iron oxide act as Lewis acids, therefore coordinate with molecules that donate lone-pair electrons. In aqueous solutions, iron atoms coordinate with water, which rapidly dissociates leaving the iron oxide surface hydroxyl

functionalized. Being the hydroxyl groups amphoteric, they may react with acids or bases. The surface of the magnetite will be positive or negative, depending on pH present in solution. The isoelectric point (also called point of zero charge, PZC) is observed at pH 6,8. Around the PZC the particles are no longer stable in water and flocculate, because their surface charge density is too low. To obtain stable iron oxide nanoparticles, it is then necessary to act on both electrostatic and steric stabilization.
Many different stabilizers were studied:

- Monomeric stabilizers, such as carboxylates, phosphates.
- Inorganic materials: silica, gold.
- Polymer stabilizers, such as dextran, polyethylene glycol (PEG), polyvinyl alcohol (PVA).

4.2 Nanocomposites for wastewater treatment

Only a few studies have been carried out on nanocomposites applied to wastewater treatment. Mahdavian et al. [21] investigated the ability of magnetite nanoparticles functionalized with APTES ((3-aminopropyl)triethoxysilane) and acryloyl chloride (AC) to adsorb heavy metal cations such as Cd^{2+}, Pb^{2+}; Ni^{2+} and Cu^{2+}. By FT-IR (Fourier Transform Infrared Spectroscopy) spectra, they found that aminosilane molecules are linked on the surface of the magnetite nanoparticles, through Fe-O-Si chemical bonds. The APTES-NPs particles can be further modified, for example with acryloyl chloride. Furthermore, metal cations concentration in solution decreased in time until being completely removed. The adsorption capacity was maximum for lead ions and minimum for cadmium ions.
Ozmen et al. [22] studied the capacity of magnetite nanoparticles functionalized with APTES and glutaraldehyde (GA) to remove Cu (II) from water. They obtained good results, reaching adsorption equilibrium in 15 minutes (Figure 4.5) and found that in this case Cu removal is pH dependent. As a matter of fact the maximum removal of Cu (II) occurred at a pH equal to 4 and 5,3. According to Ozmen et al. iron oxide nanoparticles functionalized with both APTES and GA (GA-APTES-NPs) show a better adsorption capability than particles functionalized with APTES only.

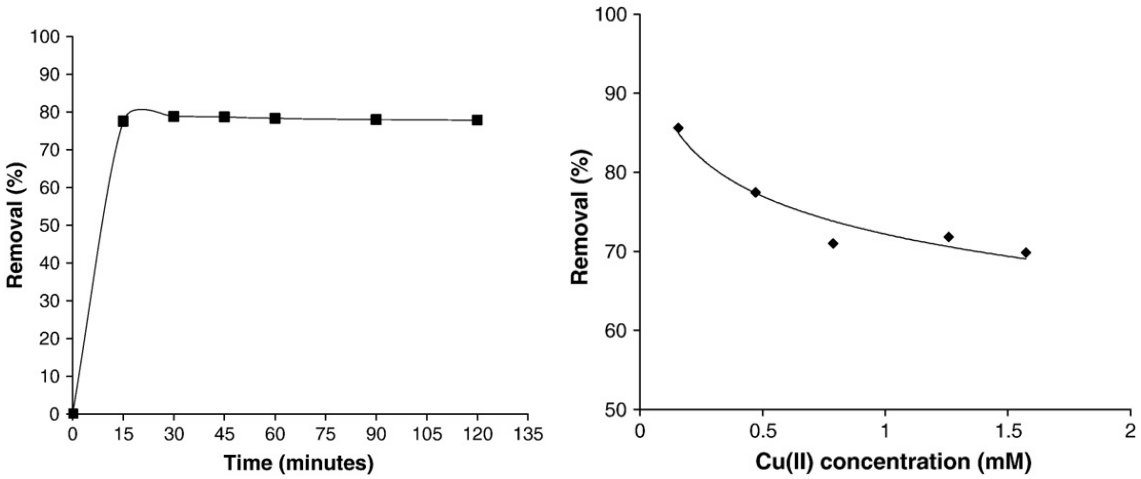

Figure 4.5: Effect of contact time (left) and initial Cu (II) concentration on the adsorbate removal by GA-APTES-NPs, synthetized by Ozmen et al. [22].

Diagboya et al. analyzed the Hg^{2+} adsorption by iron oxide nanoparticles functionalized with GO through reaction with APTES. They demonstrated that the nanocomposite adsorption capacity is five times higher than that of the pristine GO sheets. They also proved that a higher temperature has a negative effect on the process, by comparing the adsorption of Hg^{2+} at 20°C, 30°C and 40°C [23].

5. Graphene oxide

Carbon can be found in many structures ranging from diamond and graphite, that have a three-dimensional structure, to graphene (2D), nanotubes (1D) or fullerene (0D) shown in Figure 5.1. Fullerenes, nanotubes and graphite are composed of the same hexagonal array of sp^2 carbon atoms that constitutes graphene. Fullerenes and nanotubes can be represented respectively by a graphene sheet rolled in a spherical and cylindrical shape. In graphene, carbon atoms are arranged in a two-dimensional honeycomb lattice as shown in Figure 5.1. Graphite can be considered as composed of sheets of graphene shifted with respect to each other [24].

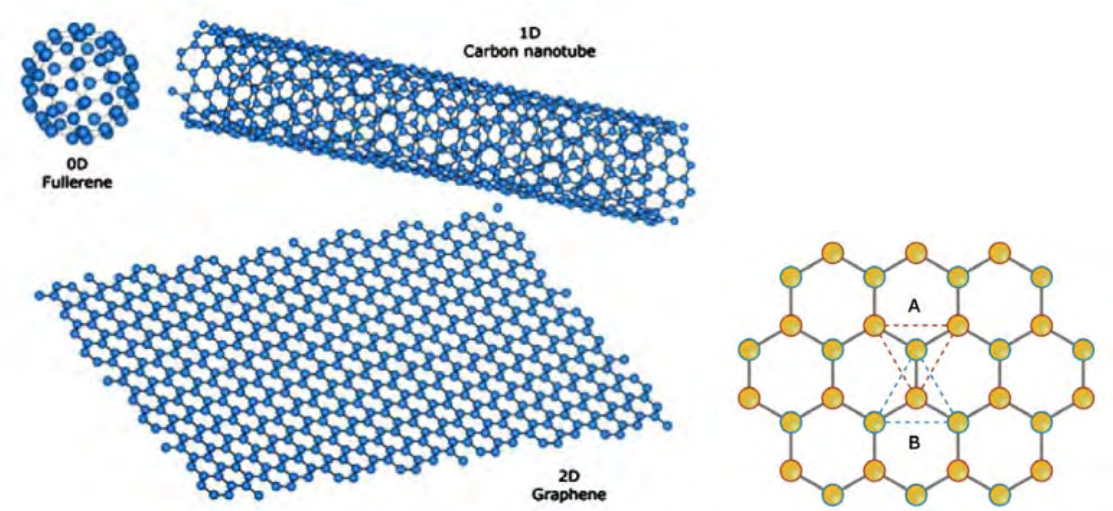

Figure 5.1: On the left three carbon allotropes structures, fullerene, carbon nanotube and graphene. On the right, the blue and the red triangles shows how graphene lattice is composed of interpenetrating triangles [24].

Graphene is becoming increasingly important in many science and technology fields because of its peculiar characteristics:

- High specific surface area.
- Electronic properties and electron transport capabilities.
- Pliability and impermeability.
- Strong mechanical strength.
- Excellent thermal and electrical conductivities.

Graphene oxide (GO, Figure 5.2) consists of a single-layer of graphite oxide and is produced by the oxidation of graphite followed by its dispersion and exfoliation in water or other suitable organic solvent. It is a precursor for graphene synthesis by chemical or thermal reduction. Its structure is not yet well known even if many oxygen-containing functional groups have been identified on both the planar surface of the sheet (mainly hydroxyl and epoxy groups) and its edges (small amounts of carboxy, carbonyl, phenol, lactone and quinone).

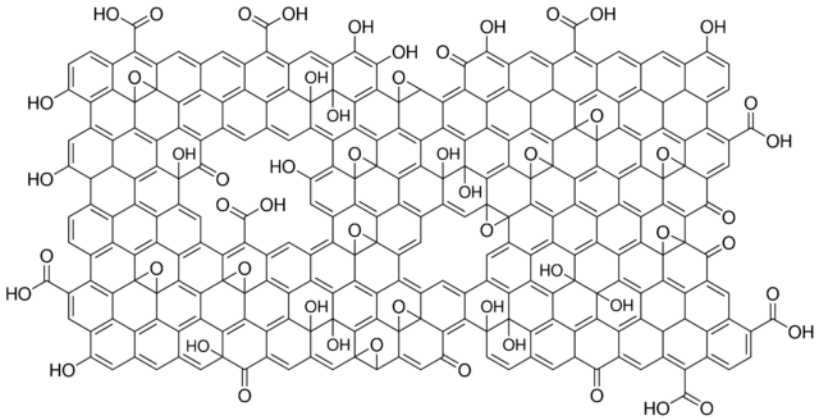

Figure 5.2: Graphene oxide, structural formula.

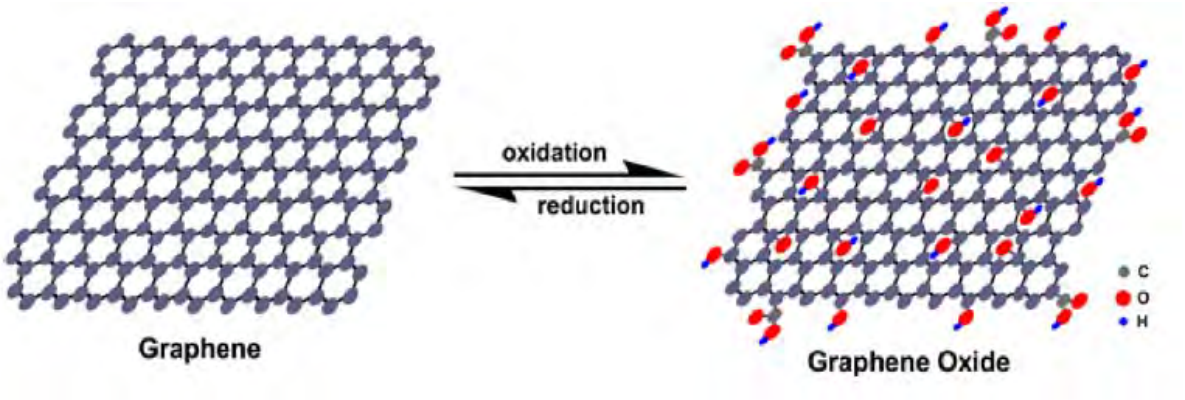

Figure 5.3: This scheme shows how GO presents oxygen-containing functional groups on both the planar surface and the edges [25].

These oxygenated groups influence GO's electronic, mechanical and electrochemical properties. For the same reason GO is characterized by some peculiar advantages and drawbacks if compared with pristine graphene [25].

The advantages gained in GO are:

- Hydrophilic structure thanks to the polar oxygen functional groups. Therefore GO is dispersible in many solvents and forms a stable colloidal dispersion in water. This effect is caused by the low acidity constant of carboxyl groups (that quickly dissociate into carboxylate anions) that characterize GO with negative surface charge up until very low pH values (<1).
- Functional groups can be used as sites to chemically modify GO. They allow to synthesize many GO composites useful to remove toxic metals from water.
- Facile synthesis.
- Unique optical properties (such as fluorescence labels).
- Lower costs of GO-based devices compared with conventional electrodes and adsorbents. GO is easily produced from graphite, that is abundant in nature and its adsorption capacities are becoming progressively similar to those of zeolites [25, 16].

Thanks to these properties many graphene and graphene oxide-based materials with great potential for environmental applications can be prepared. However a strategy for GO recovery after sorption must be developed in order to apply it to pollutants' decontamination [16]. This problem can be solved using magnetic nanoparticles.
The covalent oxygenated functional groups originate flaws on the graphene structure that cause some drawbacks in the use of GO:

- Loss in electrical conductivity [25].
- Multistep, complex procedures to synthetize composite materials that irreversibly modify GO structure.
- GO composites have narrow ranges of application.
- Difficulty in removing GO from solution.
- Oxygenated groups present on GO characterize it with in vivo toxicity [16].

5.1 Adsorption and desorption of iron oxide nanoparticles from graphene oxide

As previously stated iron oxide NPs surface chemistry depends on pH in solution and its isoelectric point (IEP) is equal to 7,48. When pH is below the IEP value, iron oxide is expected to show strong attraction to GO due to the opposed surface charges (Figure

5.4). When the pH increases above the IEP the GO can be redispersed in solution since the adsorption doesn't modify GO, making the process fully reversible.

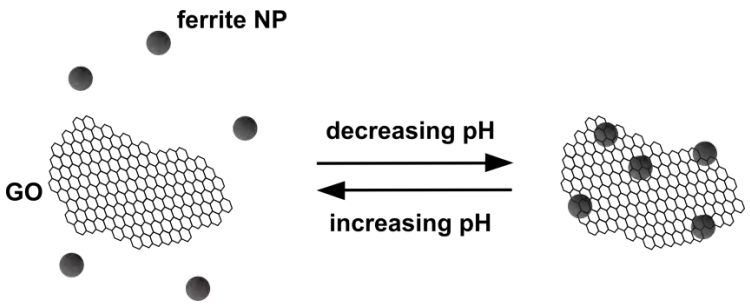

Figure 5.4: Change in attraction or repulsion forces between GO and iron oxide nanoparticles with varying pH [16].

Therefore the adsorption of magnetic substances on GO can be controlled by changing the surface charge with a pH adjustment. Once magnetic nanoparticles are attached to GO, the latter can be easily removed by water applying a magnetic field as shown in Figure 5.5. The reversibility of the process allow to reuse both GO and the magnetic material.

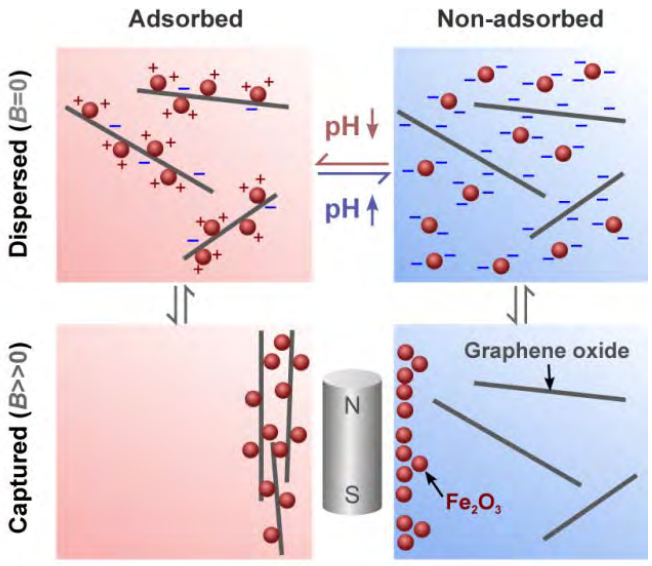

Figure 5.5: Different effect caused by the application of a magnetic field depending on pH in solution [16].

Figure 5.6 shows the isoelectric points of GO and of iron oxide, respectively equal to approximately zero and 7 (for both maghemite and magnetite). Hence the two materials have opposite surface charges for a wide pH range, in which they are expected to undergo Coulombic attraction.

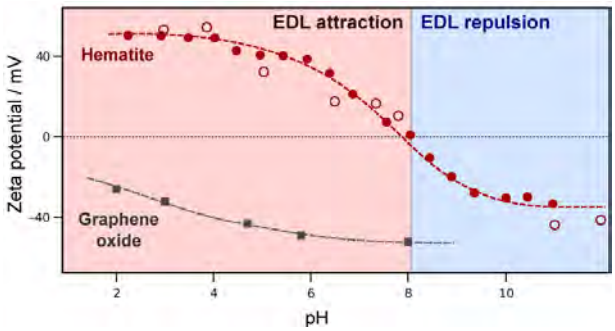

Figure 5.6: GO and iron oxide zeta potentials [16].

McCoy et al. analyzed this behavior applying iron oxide microparticles, nanoparticles and also magnetic surfactants system.

The results obtained confirmed the expected behavior. Figure 5.7 shows the narrow range of pH in which the transition between complete adsorption and dispersion of GO occurs in the case of iron oxide microparticles. At pH 12 there is a decrease in dispersed GO, likely due to the fact that GO starts to become chemically reduced [16].

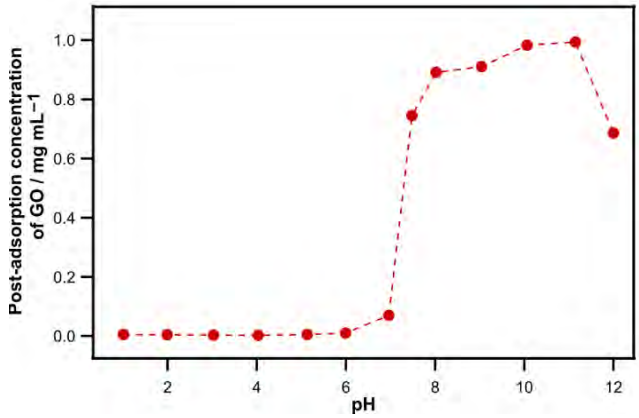

Figure 5.7: GO concentration in solution as a function of pH with a fixed initial GO concentration of 1,5 mg/ml and 20 mg of Fe_2O_3 microparticles [16].

6. Aim of the thesis

The aim of the present thesis is to syntheisze new magnetic iron oxide based nanocomposites and to study their application to heavy metals removal from stormwater. The nanocomposites are synthetized by functionalizing bare iron oxide nanoparticles and binding them to graphene oxide nanosheets. In particular, two main types of nanoadsorbents will be taken into account for the removal tests:

- Iron oxide magnetic nanoparticles (MNPs) as synthesized and with coordinating or chelating groups on the surface, specifically designed to bond heavy metal ions.

- Graphene oxide nanosheets decorated with magnetic nanoparticles. Graphene oxide has been already applied with success to the purification of water by absorption of a wide range of organic pollutants. The composites obtained by decorating it with the magnetic material will allow for his response to magnetic fields and its easy separation from the treated water. Graphene oxide will be decorated with both bare and already functionalized magnetic nanoparticles.

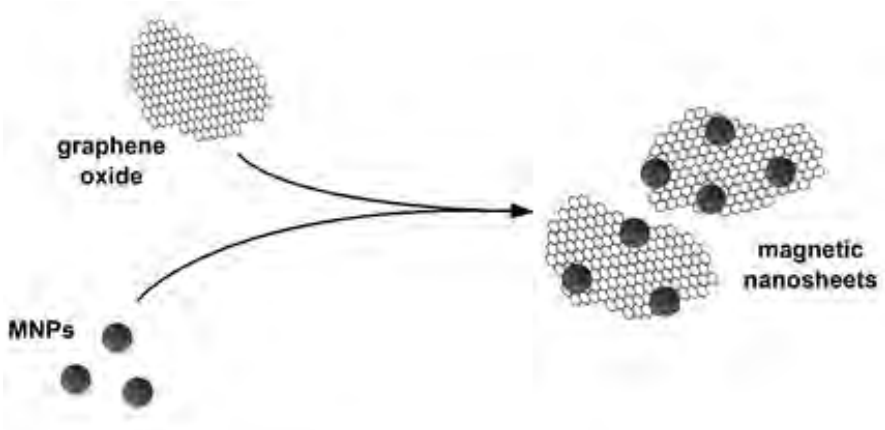

Figure 6.1: Scheme for the synthesis of the MNPs/graphene oxide composites.

The nanocomposites will be analyzed through magnetic measurements to determine the efficiency of the separation by magnet, in order to understand the viability of this removal system.

The nanocomposites will then be applied to heavy metals removal through adsorption experiments.

The metals studied are lead, chromium and nickel, all very dangerous for human health. Their toxic effects on humans are:

- Lead: damage to the fetal brain, diseases of the kidneys, circulatory system, and nervous system.
- Chromium: headache, diarrhea, nausea, vomiting. Furthermore it is carcinogenic.
- Nickel: dermatitis, nausea, chronic asthma, coughing. This metal is another human carcinogen [2].

The nanocomposites would be more efficient if applied directly to stormwater, especially considering that these are often stored in stormwater tanks to limit overloading of the sewage system. This would avoid the problems caused by high suspended matter content on the removal of heavy metals. Instead, if heavy metals must be removed in the final treatment plant, the device should be placed after a primary settler but before the activated sludge system. A device implementing the nanocomposites studied in the present thesis might be placed in the oil and fats separator or after this unit, as shown in Figure 6.2, in which A and B are the different possible positions.

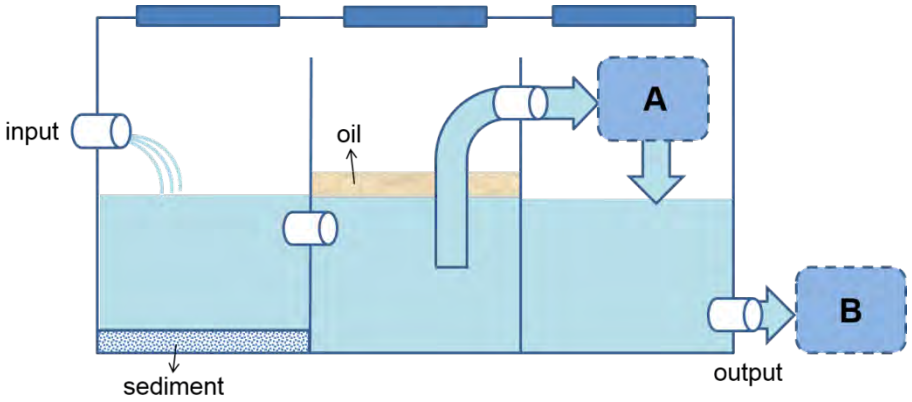

Figure 6.2: Possible positions for the device implementing nanocomposites.

The magnetic device for the nanocomposites separation includes two magnetic elements:

1. A magnetic element to stir the nanoparticles injected in the dirty water.

2. A magnet to attract the magnetic nanoparticles with the linked pollutants after treatment. The stirring of nanoparticles will be obtained using a time varying magnetic field generated by means of some permanent magnets in rotation or a coil supplied by a time varying electrical current and positioned close to the nanoparticles injection elements.

Separated magnetic nanocomposites will be directed to a recycling system, Figure 6.3. In this unit pollutants will be chemically separated and the magnetic cores will be magnetically separated by a second magnetic element, in order to recycle the nanoparticles that can be reused for a new cleaning process.

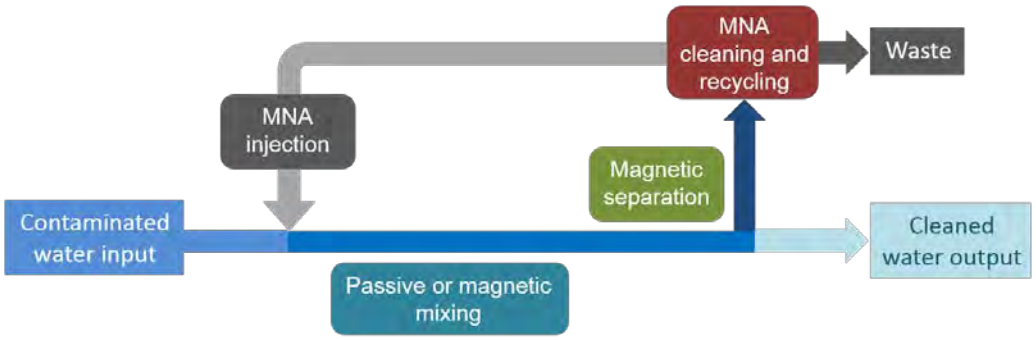

Figure 6.3: Scheme of the cleaning cycle (MNA = Magnetic Nano-Adsorbents).

7. Nanocomposites synthesis and functionalizations

Different nanocomposites are synthetized and applied to water treatment in this study. There are two main types of nanocomposites studied Table 7.1. To the first class belong nanocomposites without GO. These are bare nanoparticles (NPs) and NPs functionalized with:

- 3,4-dihydroxyhydrocinnamic acid, DHCA
- Caffeic acid, CA
- (3-Aminopropyl)triethoxysilane, APTES

To the second class belong nanocomposites implementing GO. These are NPs functionalized with:

- Graphene Oxide, GO
- GO and DHCA
- GO and CA
- GO and APTES

Therefore nanocomposites synthetized are summarized in the following table (Table 7.1).

Table 7.1: Nanocomposites synthetized and applied to water treatment in the present study.

Nanocomposites without GO	**Nanocomposites with GO**
NPs	NPs-GO
NPs-DHCA	NPs-GO-DHCA
NPs-CA	NPs-GO-CA
NPs-APTES	NPs-GO-APTES

Chemicals used in the synthesis processes are listed in Table 7.2. All reagents were used as purchased.

Table 7.2: Chemicals used in the synthesis and functionalization of the nanocomposites.

Chemicals used	**Company furnishing the chemicals**
3,4-dihydroxyhydrocinnamic acid (DHCA, 98%)	Sigma-Aldrich
Caffeic acid (98%)	Sigma-Aldrich
(3-Aminopropyl)triethoxysilane (APTES, 98%)	Fluka
NaOH (98%)	Sigma-Aldrich
THF (99,9%)	Sigma-Aldrich
Expanded graphite, ECOPHIT 50	ECOPHIT
$KMnO_4$	Sigma-Aldrich
H_2SO_4 (98%)	Sigma-Aldrich
HCl (37%)	Sigma-Aldrich

7.1 Iron NPs synthesis

The nanoparticles used in this study are synthetized with the coprecipitation method, a very common and efficient method, although generating particles with a broader size range with respect to other techniques.
In a three neck flask were placed:

- 5 g of Iron (II) chloride tetrahydrate $FeCl_2 \cdot 4H_2O$, 25 mmol.
- 13,5 g of Iron (II) chloride esahydrate $FeCl_3 \cdot 6H_2O$, 50 mmol.
- 150 ml of deionized water.

While the flask is undergoing mechanical stirring, 12,5 ml of ammonium hydroxide solution (NH_4OH) are added. The reaction occurring is:

$$2FeCl_3 \cdot 6H_2O_{(s)} + FeCl_2 \cdot 4H_2O_{(s)} + 8NH_4OH_{(aq)} \rightarrow Fe_3O_{4(s)} + 8NH_4Cl_{(aq)} + 20H_2O_{(l)}$$

The solution turns rapidly to a dark brown color. Ammonium hydroxide is added dropwise until obtaining a pH of 11. Then the system is heated at 60°C and 7,5 ml of oleic acid (5% v/v) are added. The synthesis' last step is mechanical stirring at 60°C for 30 minutes.

7.2 NPs-DHCA synthesis

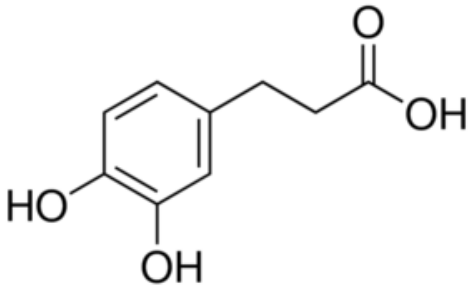

Figure 7.1: 3,4-dihydroxycinnamic acid.

The functionalization of bare nanoparticles with 3,4-dihydroxyhydrocinnamic acid (DHCA, Figure 7.1) follows the procedure presented in Liu et al. [26].
51,1 mg of 3,4-dihydroxyhydrocinnamic acid (DHCA) were dissolved in 11 ml of THF in a two-neck flask by magnetic stirring. The solution obtained was heated up to 50°C under nitrogen flow. Then 3 ml of distilled water containing 21 mg of NPs were added dropwise. The solution was cooled to room temperature after two hours. 0,5 ml of NaOH (0,5 M) were added to precipitate the magnetic nanoparticles in solution. After centrifugation (3000 rpm/min for 5 minutes, centrifuge used: Awel MF 20) the precipitate was redispersed in 2 ml of distilled water.

7.3 NPs-CA synthesis

Functionalization with 3,4-dihydroxyhydrocinnamic acid or caffeic acid is obtained with the same procedure given the high similarity between the two acids (Figure 7.2).

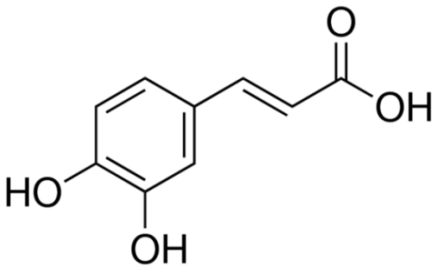

Figure 7.2: Caffeic acid structural formula.

51,1 mg of caffeic acid were dissolved in 11 ml of THF in a two-neck flask by magnetic stirring. The solution obtained was heated up to 50°C under nitrogen flow. Then 3 ml of distilled water containing 21 mg of NPs were added dropwise. The solution was cooled to room temperature after two hours. 0,5 ml of NaOH (0,5 M) were added to precipitate the magnetic nanoparticles in solution. After centrifugation (3000 rpm/min for 5 minutes) the precipitate was redispersed in 2 ml of distilled water.

7.4 NPs-APTES synthesis

The nanocomposite used in the present study were functionalized with APTES ((3-aminopropyl)triethoxysilane), following the same procedure presented by Mahdavian et al.

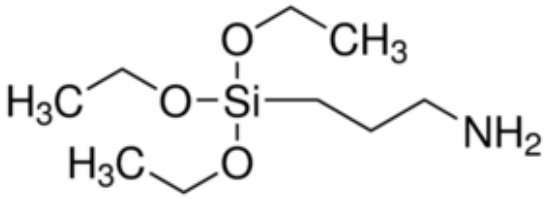

Figure 7.3: (3-Aminopropyl)triethoxysilane structural formula.

20 ml of nanoparticles in distilled water were centrifuged (10000 rpm for 10 minutes) and washed with ethanol twice. Then 140 mg of nanoparticles in ethanol underwent 30 minutes of sonication before the addition of 4,3 g of APTES. After stirring for 7 hours at room temperature the material was separated by centrifugation (10000 rpm for 10 minutes) and washed with ethanol three times. Finally the product was vacuum dried under N_2 gas.

7.5 Graphene oxide synthesis

Graphene oxide used in this study was obtained with a modified Sun method [27] by Doctor Flavio Pendolino and Professor Roberta Bertani.

5 g of expanded graphite and 15 g of potassium permanganate were placed in a 1l beaker and stirred to obtain homogeneity. While stirring continued, the beaker was placed in an ice−water bath, and 100 ml of concentrated sulfuric acid (98%) was added slowly (since the reaction is exothermic) until obtaining a petrol-green liquid paste. Then, the system was kept at room temperature with continuous stirring until a foam-like material was formed (about 20 min were needed). At this stage, a safety measure must be carried out: the foam material, which has density gradients, is stirred to homogeneity in order to avoid possible explosions after water addition (exothermic reaction). Then the beaker was placed again in the ice−water bath, and 400ml of distilled water was added to it very slowly (also in this case to avoid an uncontrolled temperature increase). The green-brownish liquid was then placed in a 90°C water bath for 1 h and a dark suspension was obtained. The suspension was paper filtered and then underwent washings with the following subtances:

1. 500 ml of distilled water.
2. 200 ml of HCl 5% to remove manganese
3. 500 ml of distilled water.

7.6 NPs-GO synthesis

The iron oxide/GO nanocomposites are synthetized following the procedure in Kyzas et al. [28] using:

- 4 ml of distilled water containing 28 mg of iron oxide nanoparticles.
- 28 mg of GO.
- 24 ml of distilled water.

The dispersion obtained undergoes 30 minutes of sonication, then the nanocomposites are collected by magnetic separation. After most water is collected with a pipette, distilled water is added and the dispersion is sonicated again for 5 minutes. These last

three steps are repeated another time. Finally, after magnetic separation, the nanocomposites are vacuum dried under nitrogen gas.

7.7 GO nanocomposites

The procedure presented in paragraph 7.6 was applied to iron oxide nanoparticles functionalized with DHCA, Caffeic acid, and APTES. The following figure (Figure 7.4) shows the main steps of the procedure to obtain iron oxide NPs functionalized with APTES and GO. The first part of the synthesis follows the same steps of the NPs-APTES synthesis. In the second part GO is linked by sonication. APTES and GO are linked by a covalent bond as demonstrated by Diagboya et al. [23].

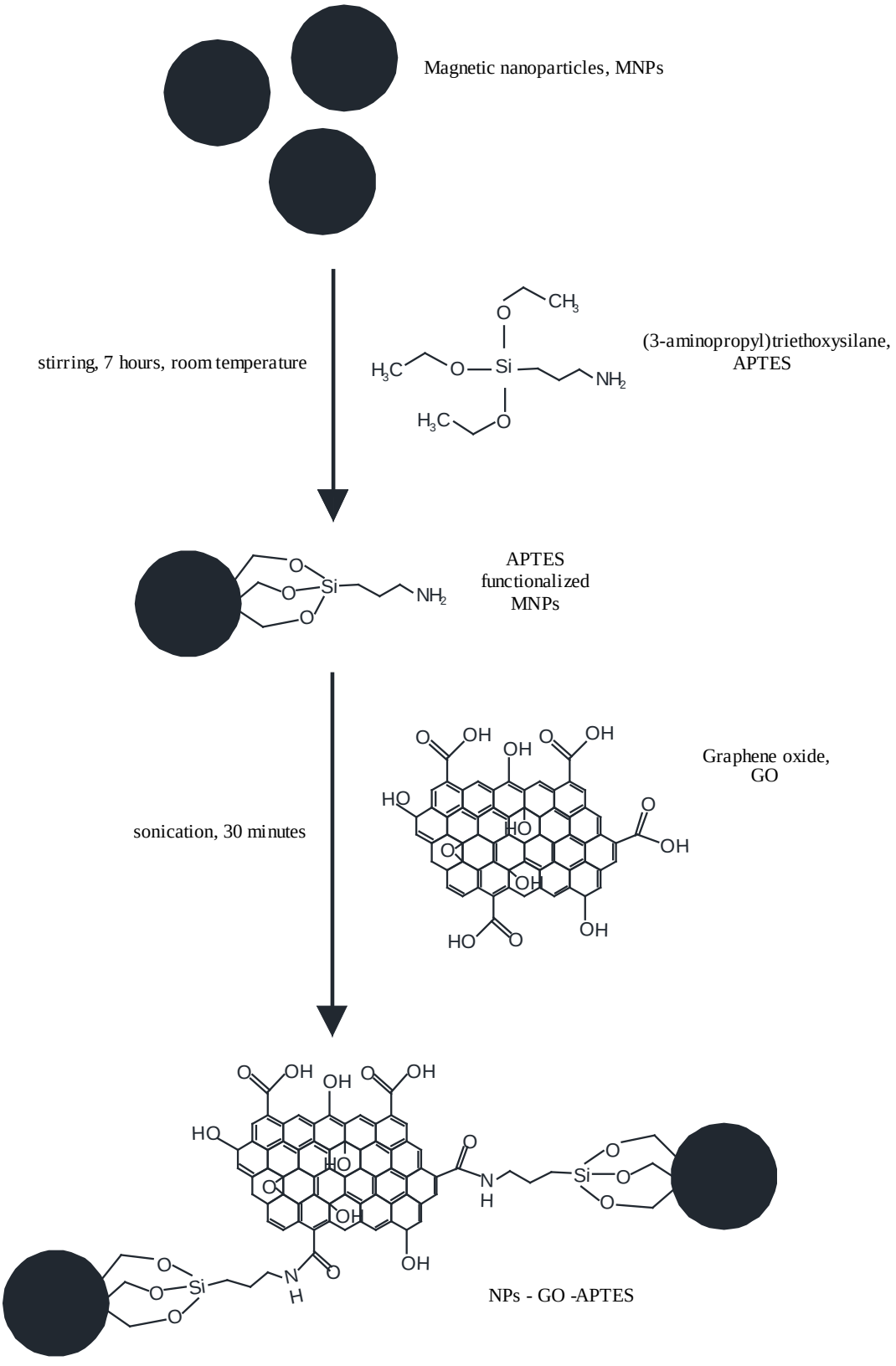

Figure 7.4: Main steps of the functionalization of iron oxide nanoparticles with APTES and graphene oxide.

8. Vibrating Sample Magnetometer

Magnetic properties of materials can be detected by measuring a change in magnetic flux, force, or by indirect techniques. Magnetic measurements shown in this study were carried out by Doctor Sara Laureti in the laboratory of "Materiali Magnetici Nanostrutturati" at the "Istituto di Struttura della Materia (CNR)" in Rome (Italy).
The magnetometer used is a Vibrating Sample Magnetometer (VSM) detecting magnetic flux variation due to the sample displacement in a pick-up coil system. This device, invented 40 years ago, allows to take fast magnetic measurements.
Figure 8.1 shows a simplified scheme of a magnetometer. The procedure is the following [29]:

1. The loudspeaker assembly causes the sample to vibrate perpendicularly to the applied field.
2. The oscillating magnetic field of the vibrating sample induces a voltage in the stationary detection coils.
3. The magnetic properties of the sample are deduced from measurements of this voltage.
4. A second voltage is induced in a similar stationary set of reference coils by a reference sample (a small permanent magnet or an electromagnet).
5. Since the sample and the reference are driven synchronously by a common member, the phase and amplitude of the resulting voltages are directly related.

The magnetic moment is proportional to the known portion of the voltage from the reference coils, phased to balance the voltage from sample coils.
Thanks to this procedure the measurements can be made insensitive to:

- Changes of vibration amplitude.
- Vibration frequency.
- Small magnetic field instability.

- Amplifier gain.

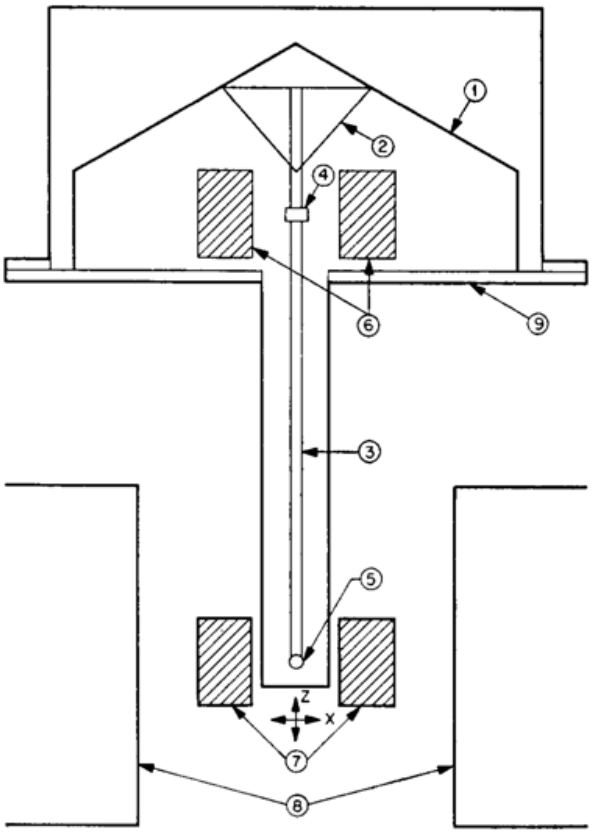

Figure 8.1: Simple scheme of the vibrating sample magnetometer: (1) loud-speakers transducer, (2) conical paper cup support, (3) drinking straw, (4) reference sample, (5) sample, (6) reference coils, (7) sample coils, (8) magnet poles, (9) metal container.

The device used for the measurements presented in this thesis is a Model 10 ADE-Technologies VSM magnetometer (Figure 8.2). It is composed of a rotating electromagnet that can generate a maximum field of 20 kOe, while the minimum detectable signal is about 20 μemu.

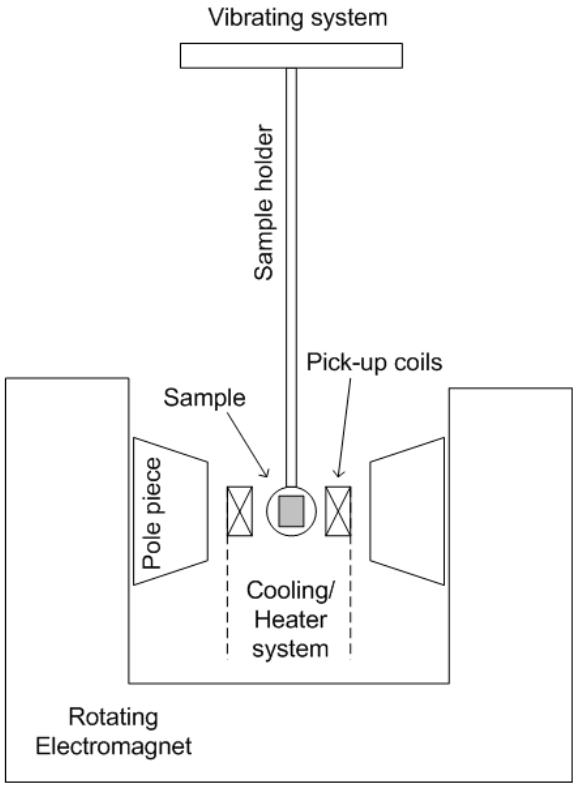

Figure 8.2: Scheme of the model 10 ADE-Technologies VSM magnetometer.

The magnetic signal is detected by 8 coils, forming 4 pairs of two coils each (Figure 8.3). Two coils assembled one over the other form a pair of coils. Two pairs of coils connected together and parallel to each other measure the signal in one direction. The other two pairs, assembled with orthogonal direction to the first ones, measure the magnetic signal in the perpendicular direction with respect to the first direction.

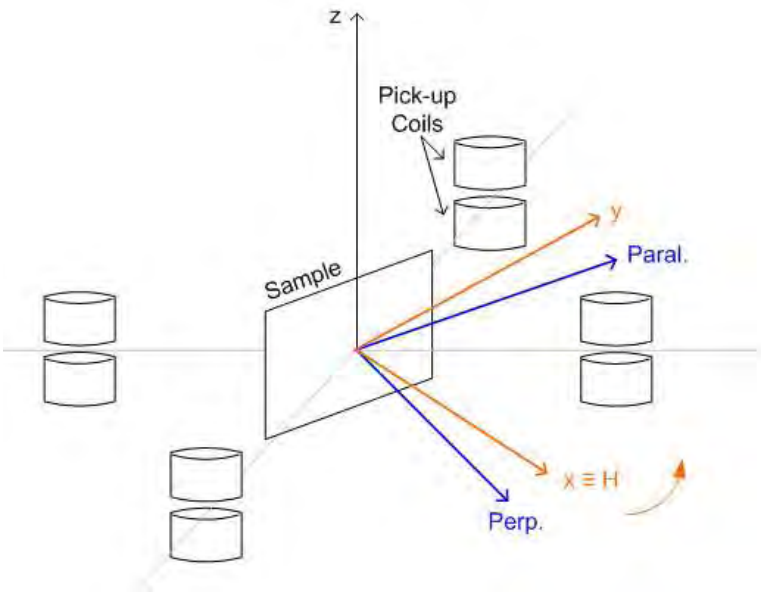

Figure 8.3: VSM setup.

These setup allow rotation and vector option and consequently allow:

- Angle dependent measurements.
- Magnetic anisotropy measurements.
- Determination of the intrinsic magnetic behavior.

9. Adsorption experiments

Heavy metals have different adverse health effect, therefore, as previously explained, it is important to limit their spreading in the environment. In this study the removal of three metals is analyzed, chosen because of their serious effects on human health, such as chronic asthma or illnesses of the nervous system.

- Lead
- Chromium
- Nickel

These metals are between the most hazardous to the environment.
In the adsorption experiments, the following procedure was followed for each type of nanocomposite synthetized. 20 ml of solution of each metal containing 20 mg of nanoparticles were magnetically stirred for two hours.
Then the nanoparticles were magnetically separated and the solution was centrifuged. 15 ml were collected, diluted to obtain a volume equal to 100 ml and analyzed by ICP (Inductively Coupled Plasma). The measure was carried out with a Perkin Elmer Optima 4200 DV ICP-OES, by Doctor Sandon Annalisa the DII Department (Dipartimento di Ingegneria Industriale, Laboratori di Voltabarozzo, University of Padova). Some samples showed a light yellow color therefore needed filtration and acidification to remove the iron salts in solution before being analyzed by ICP. The most commonly known ICP is ICP-MS (Inductively Coupled Plasma Mass Spectrometry, Figure 9.1).

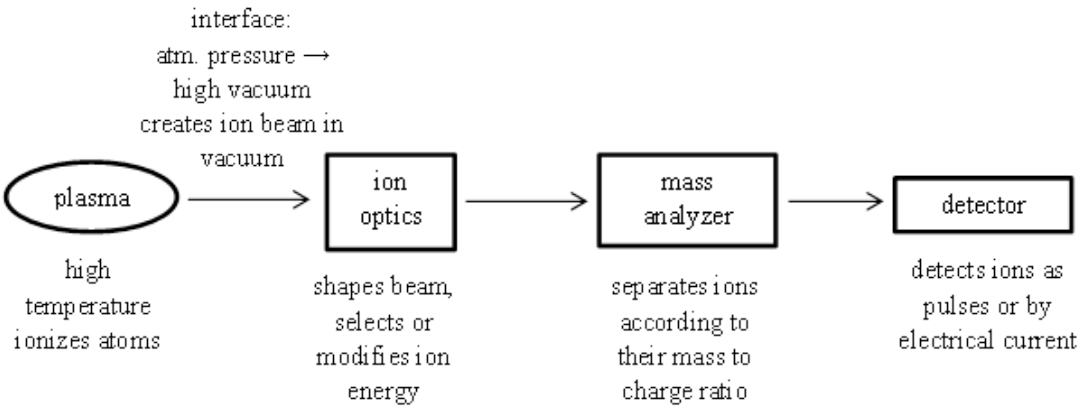

Figure 9.1: ICP-MS scheme [30].

Samples were analyzed in this study by ICP-OES (Inductively Coupled Plasma Optical Emission Spectrometry). In this process, argon gas becomes inductively coupled. This means that the moving electrons and nuclei are ripped apart in opposite directions by the magnetic field forming a plasma (a "gas" of electrons and positively charged argon ions). This plasma has a very high temperature, on the order of 5000-10000 Kelvin and emits an intense light rich in ultra-violet radiation, capable of ionizing almost all elements with high efficiency.

The samples must be injected into the plasma as:

- Gas.
- Mist.
- Fine particles (< 10 μm).

The ions jump back to their ground state, emitting photons of characteristic wavelengths. Metals present in the sample are therefore evaluated by observing these photons through a spectrophotometer [30]. This last step is the basis of ICP-OES.

10.Nanocomposites morphology

TEMs of all nanocomposites were taken in the laboratory of electron microscopy (department of Biology, university of Padova) by Doctor Federico Caicci.
As shown in the following pictures all nanocomposites have irregular, spherical-like shapes.

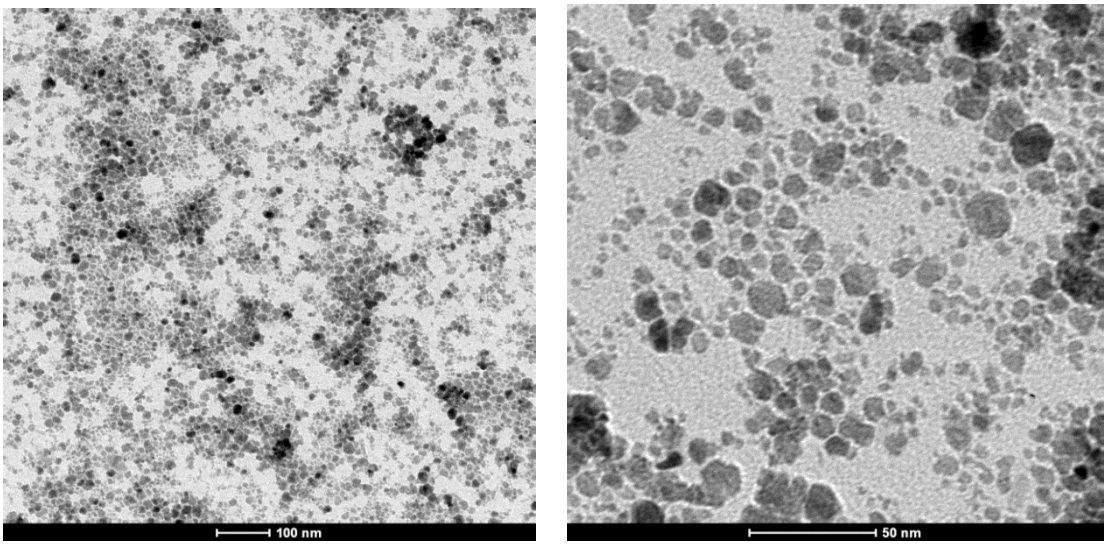

Figure 10.1: TEMs of bare iron oxide nanoparticles.

The size of the different nanoparticles ranges from 10 to 30 nm. Figure 10.2 shows some TEMs (Transmission Electron Microscopy) of DHCA functionalized nanoparticles.

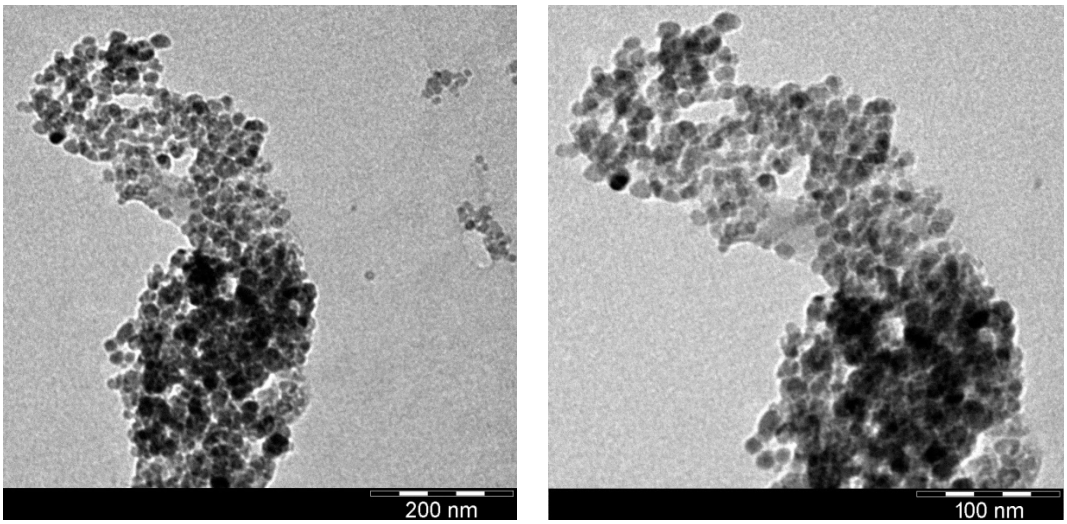

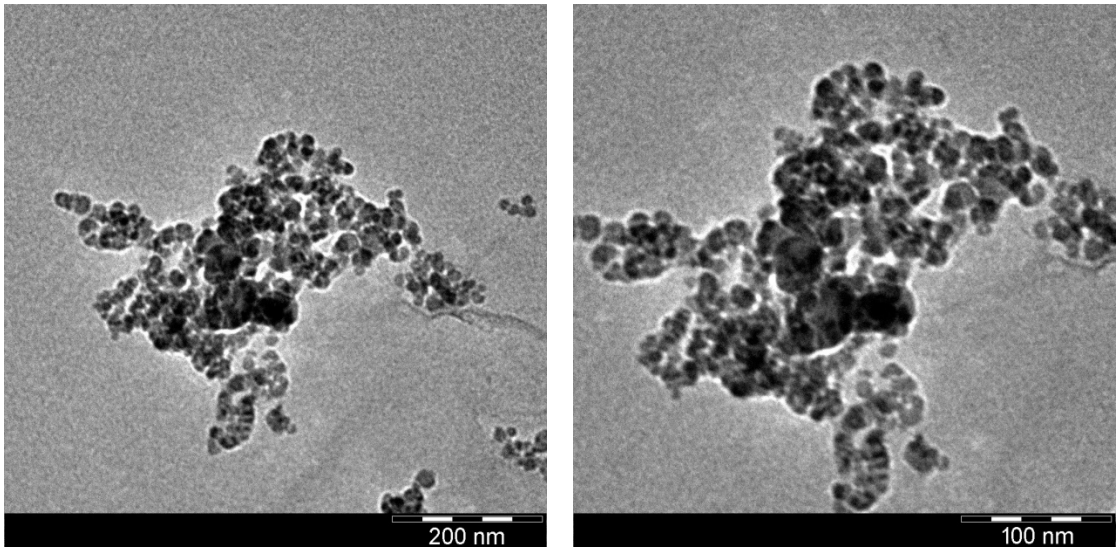

Figure 10.2: TEMs of iron oxide nanoparticles functionalized with 3,4-dihydroxycinnamic acid.

Figure 10.3 shows some TEMs of nanoparticles functionalized with caffeic acid.

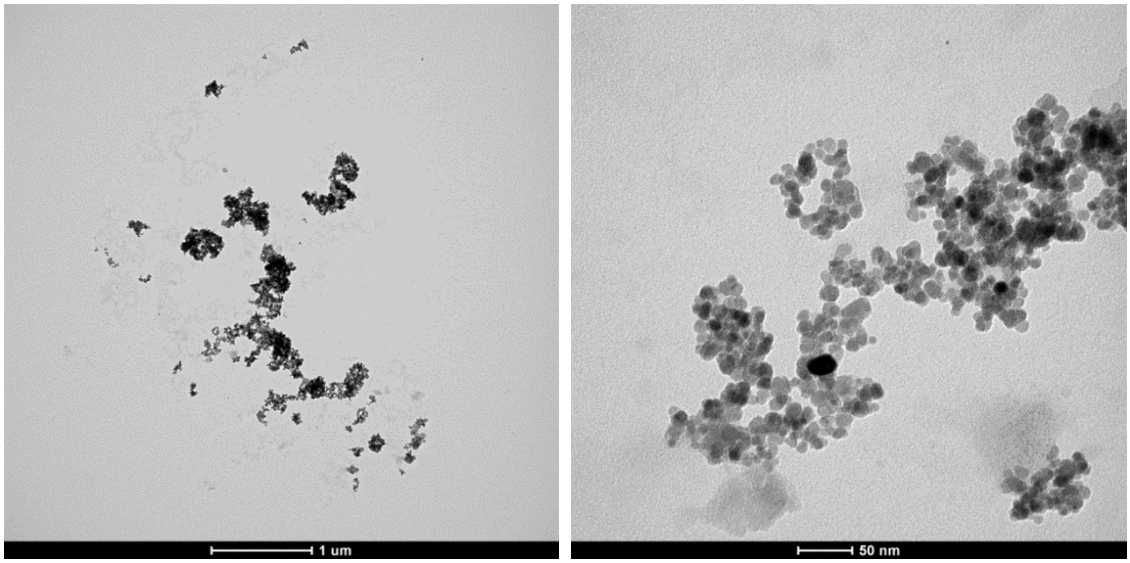

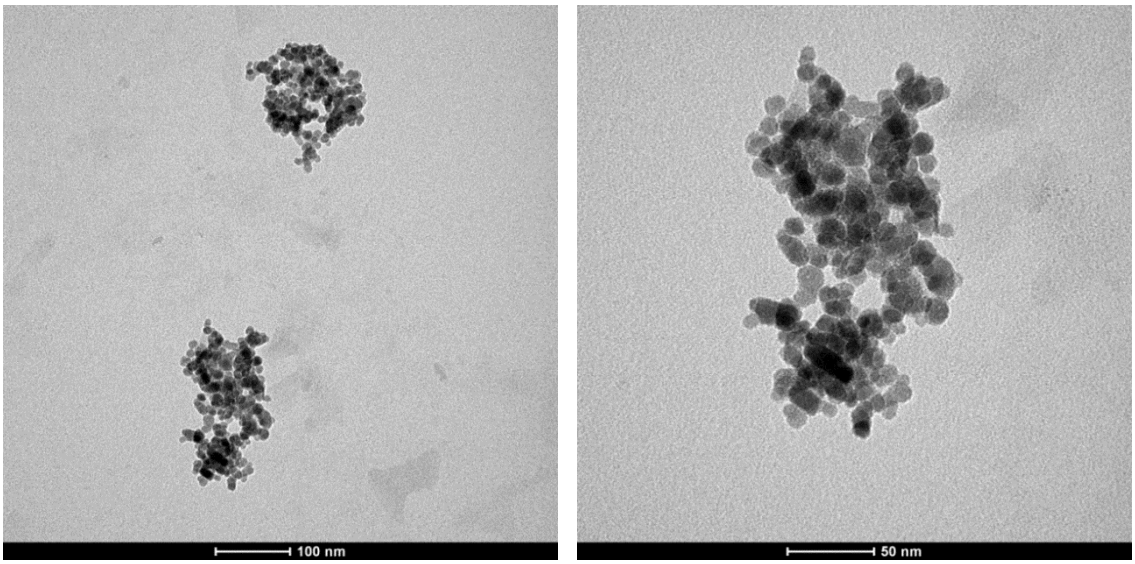

Figure 10.3: TEMs of iron oxide nanoparticles functionalized with caffeic acid.

The following pictures (Figure 10.4) are TEMs of the APTES-NPs.

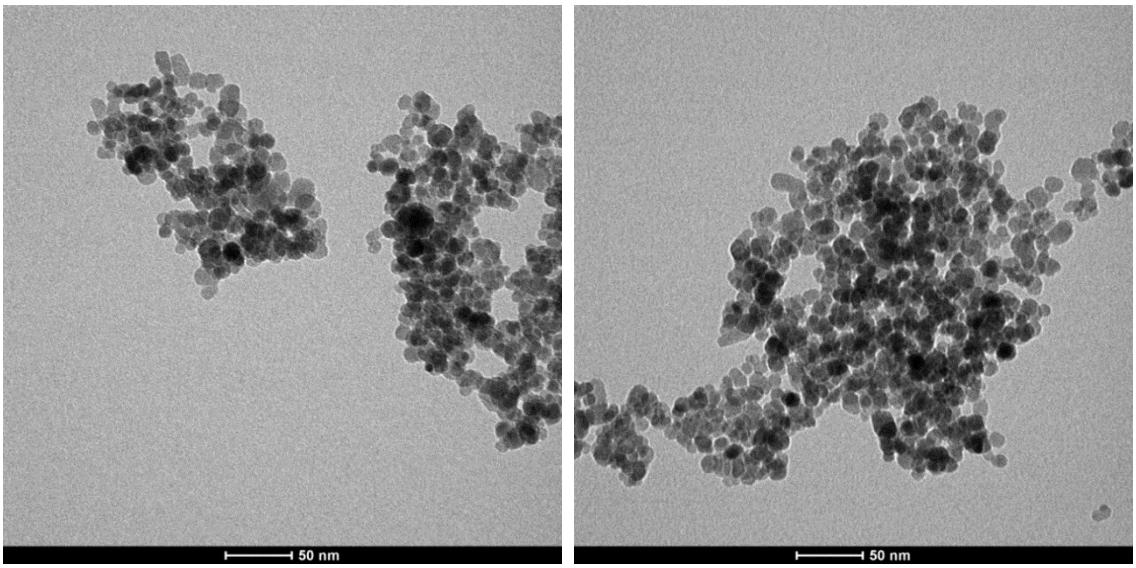

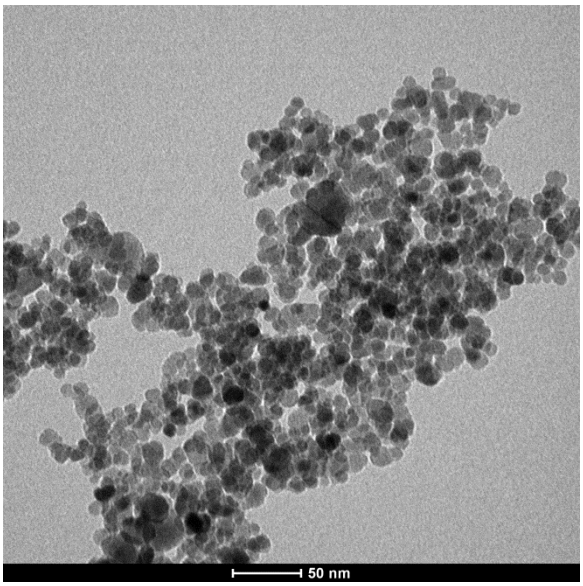

Figure 10.4: TEMs of iron oxide nanoparticles functionalized with APTES.

A TEM of GO-NPs nanocomposites are shown in the following picture (Figure 10.4).

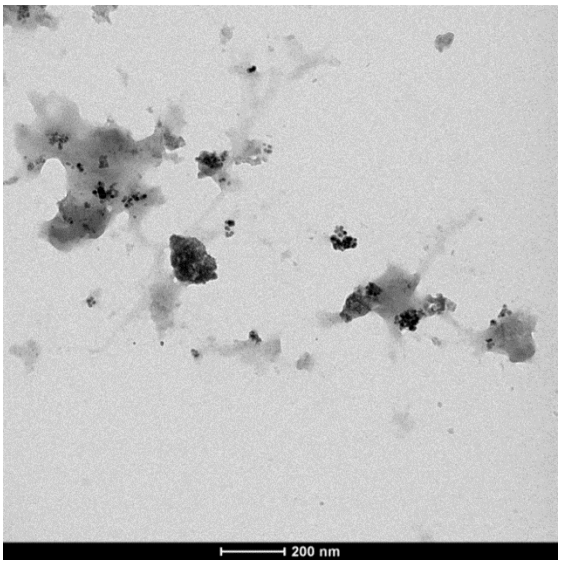

Figure 10.5: TEMs of iron oxide nanoparticles functionalized with GO.

The following pictures (Figure 10.6) show GO-DHCA-NPs. GO sheets are clearly visible in the first of the following TEMs, captured at the microscale level. As can be seen in the first TEM, graphene oxide supports the nanoparticles, therefore improving their magnetic separation efficiency after water treatment.

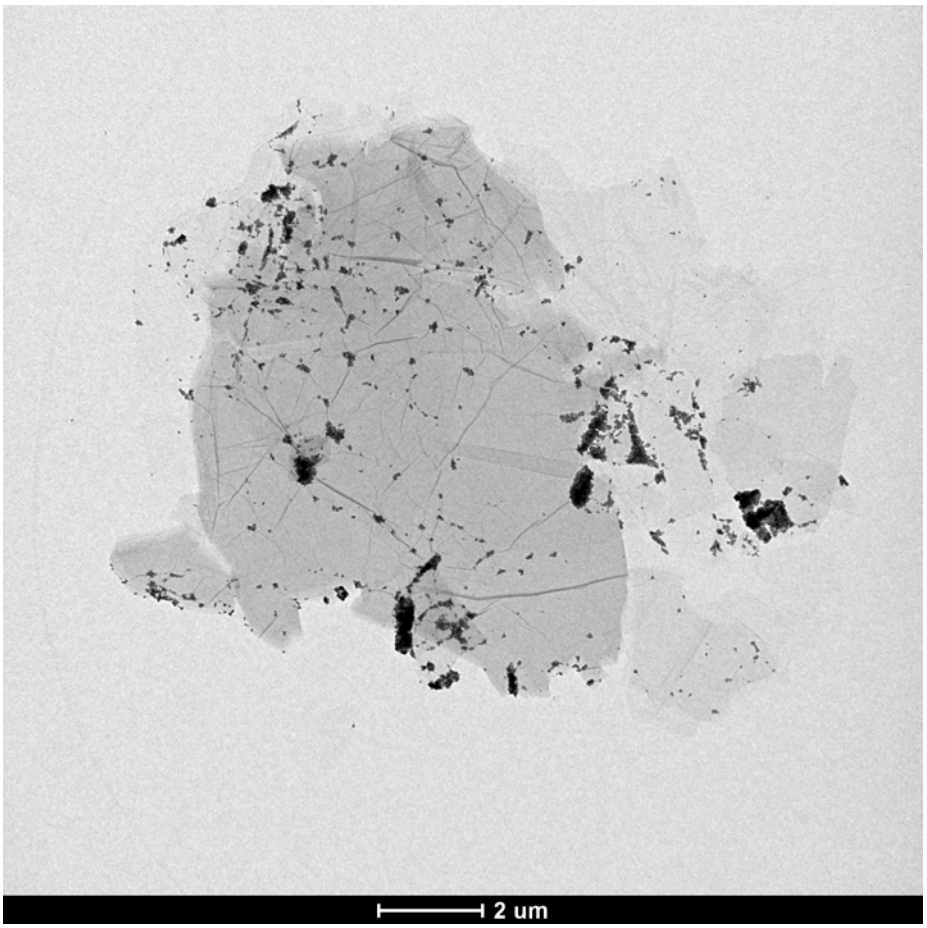

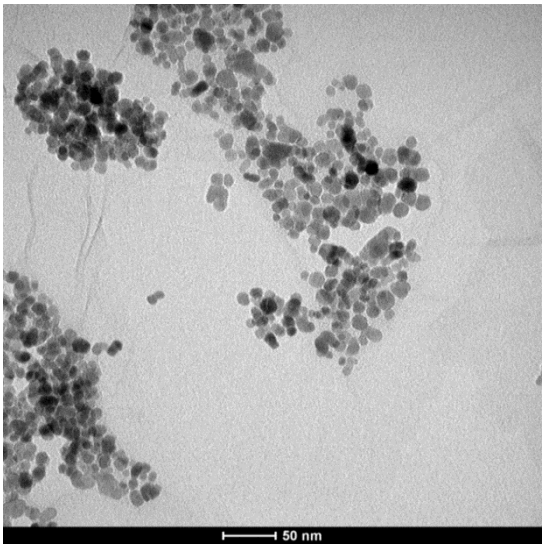

Figure 10.6: TEMs of iron oxide nanoparticles functionalized with 3,4-dihydroxyhydrocinnamic acid and graphene oxide.

The following pictures (Figure 10.7) show TEMs of iron oxide nanoparticles functionalized with caffeic acid and further modified by addition of GO (GO-Caffeic acid-NPs).

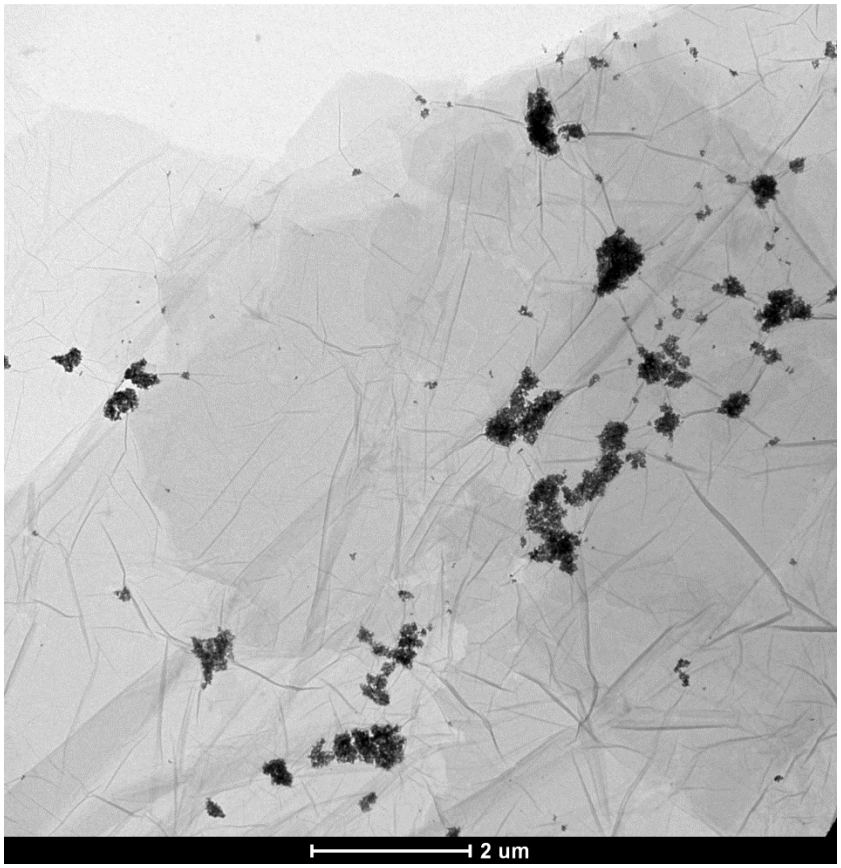

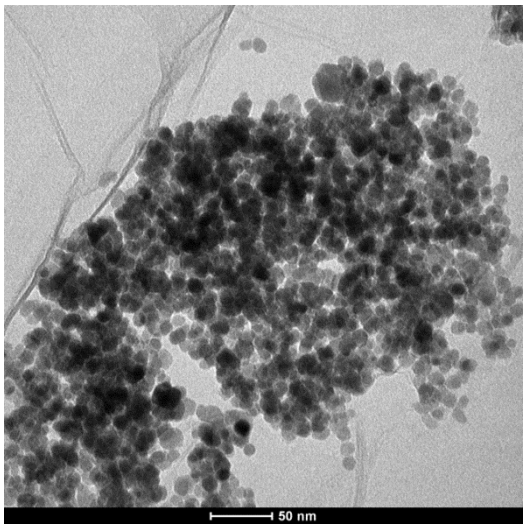

Figure 10.7: TEMs of iron oxide nanoparticles functionalized with caffeic acid and graphene oxide.

Figure 10.8 shows TEMs of GO-APTES-NPs.

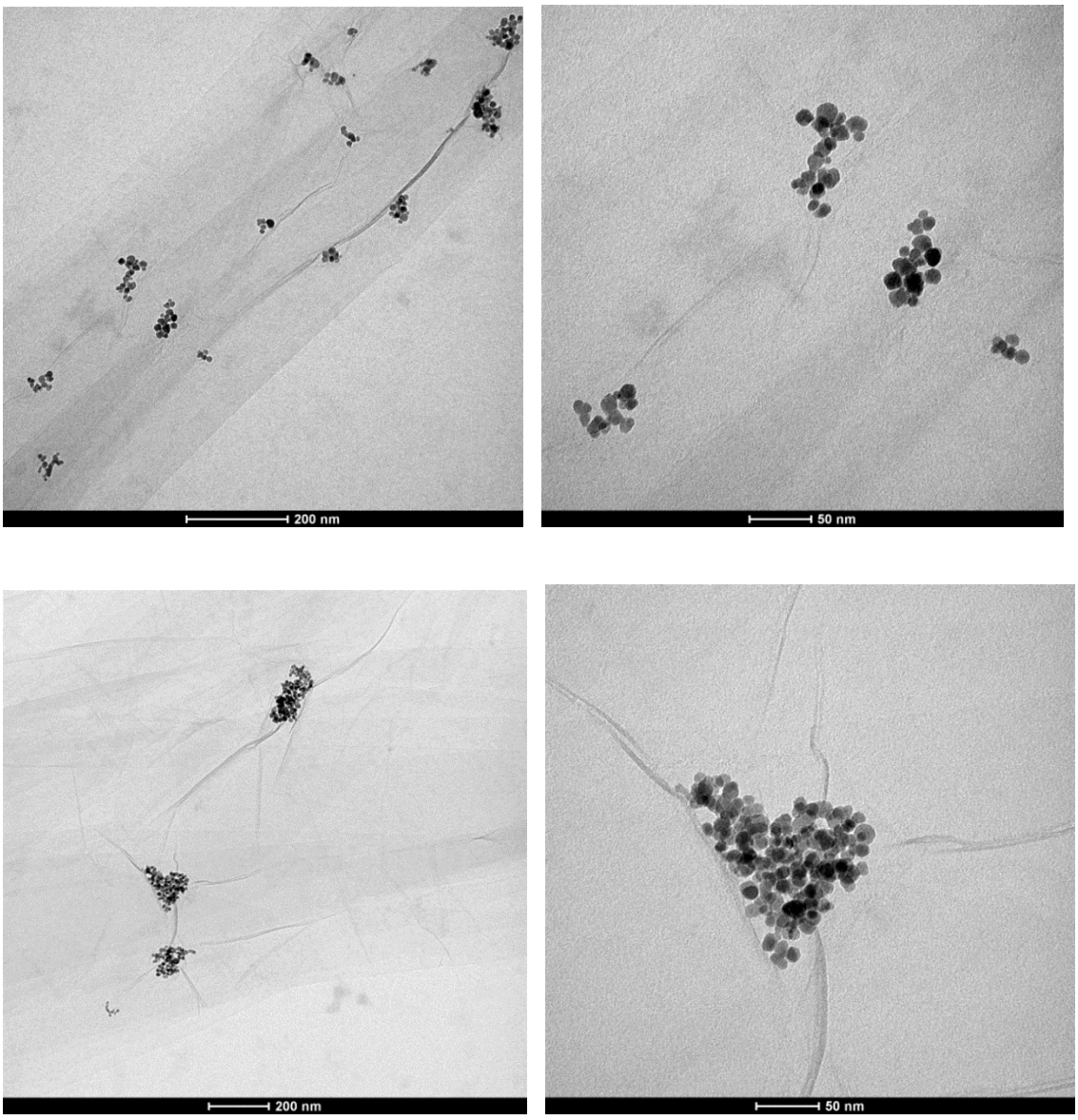

Figure 10.8: TEM of nanoparticles attached on graphene oxide sheets using APTES and GO.

11. Magnetic measurements

There are two main differences between bulk and nanoscale material. The first, as previously explained, is due to the transition of iron oxide from the ferromagnetic to the superparamagnetic state when reaching the nanoscale. The second difference is that nanoparticles may be less magnetic with respect to bulk material because on their crystal surface there is a substantially greater fraction of metal ions, which may not contribute to the particle's net magnetization [31].

As can be seen in the following graphs (Figure 11.1) the coercivity of all the nanoparticles synthetized is equal to zero meaning that they are superparamagnetic, as expected. Therefore nanoparticles are stable, they did not aggregate and they maintain their properties in time.

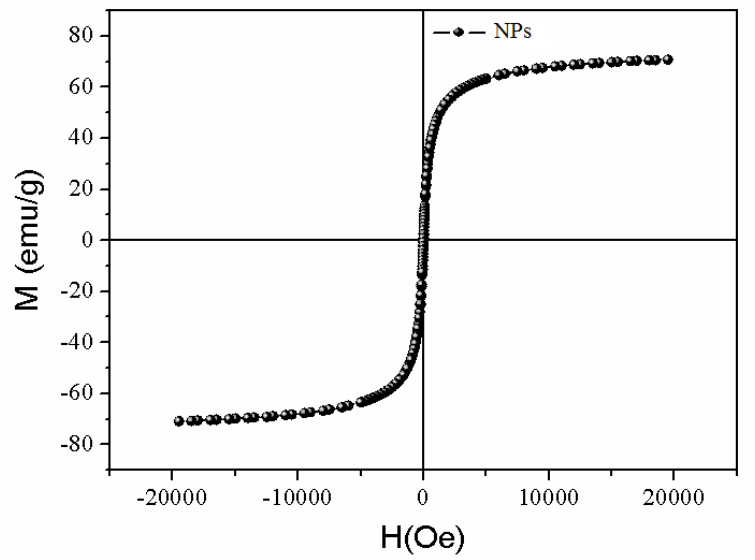

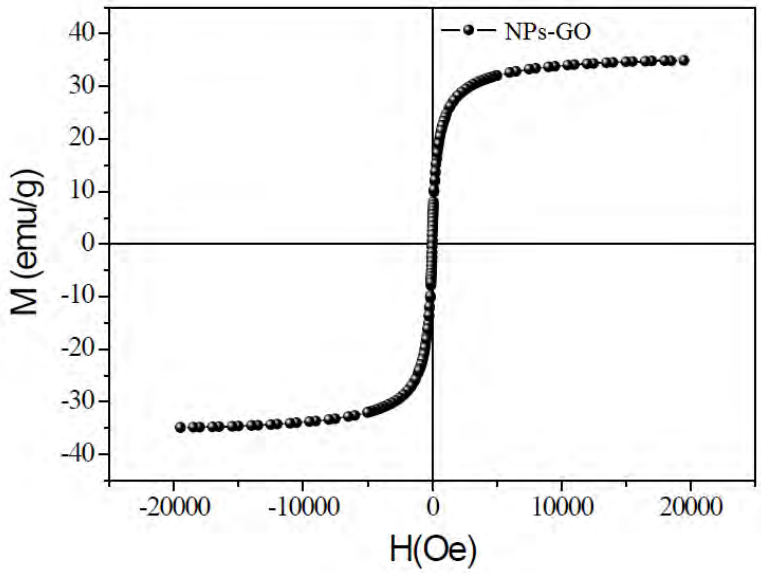
NPs-GO
M (emu/g)
H(Oe)
40
30
20
10
0
-10
-20
-30
-40
-20000
-10000
0
10000
20000

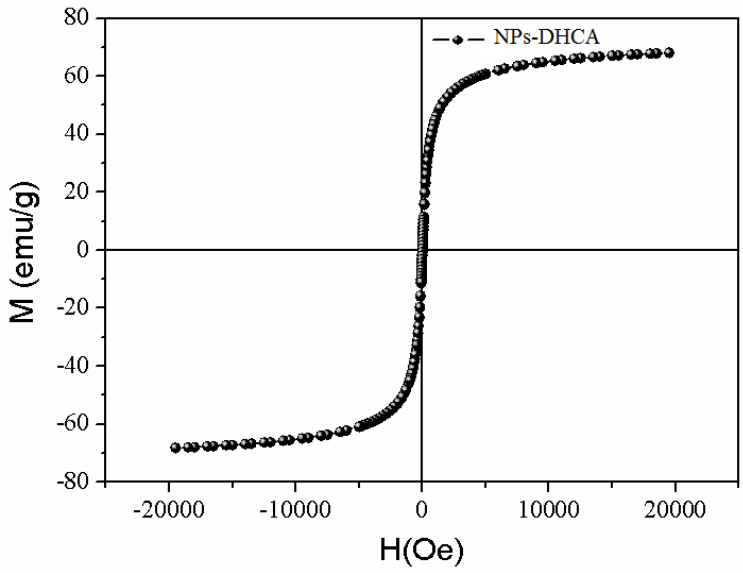
NPs-DHCA
M (emu/g)
H(Oe)
80
60
40
20
0
-20
-40
-60
-80
-20000
-10000
0
10000
20000

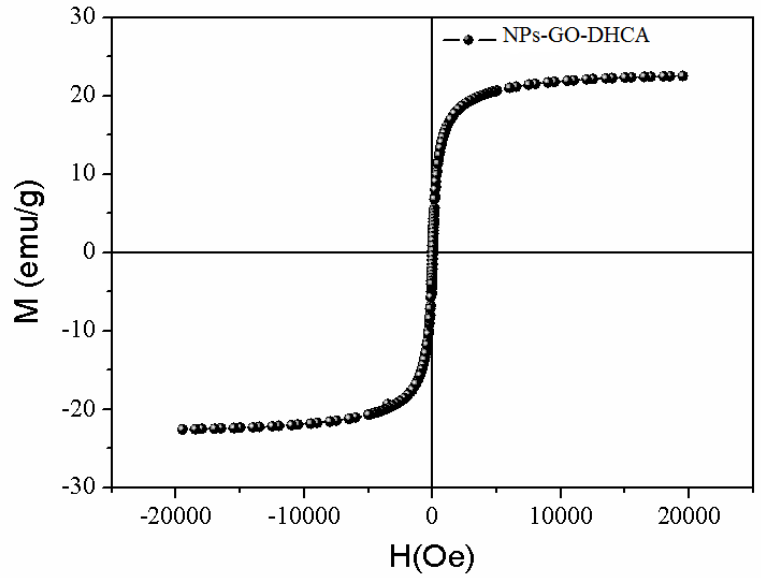
NPs-GO-DHCA
M (emu/g)
H(Oe)
30
20
10
0
-10
-20
-30
-20000
-10000
0
10000
20000

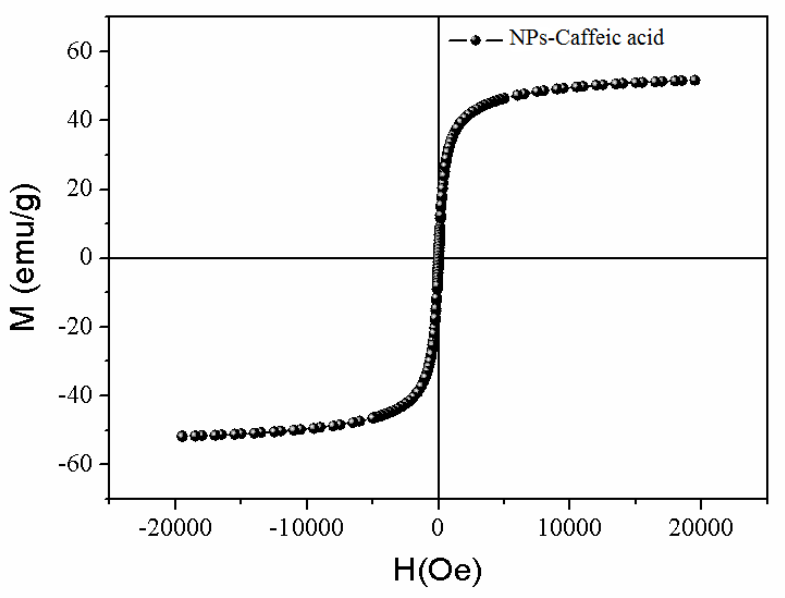
NPs-Caffeic acid
M (emu/g)
H(Oe)
60
40
20
0
-20
-40
-60
-20000
-10000
0
10000
20000

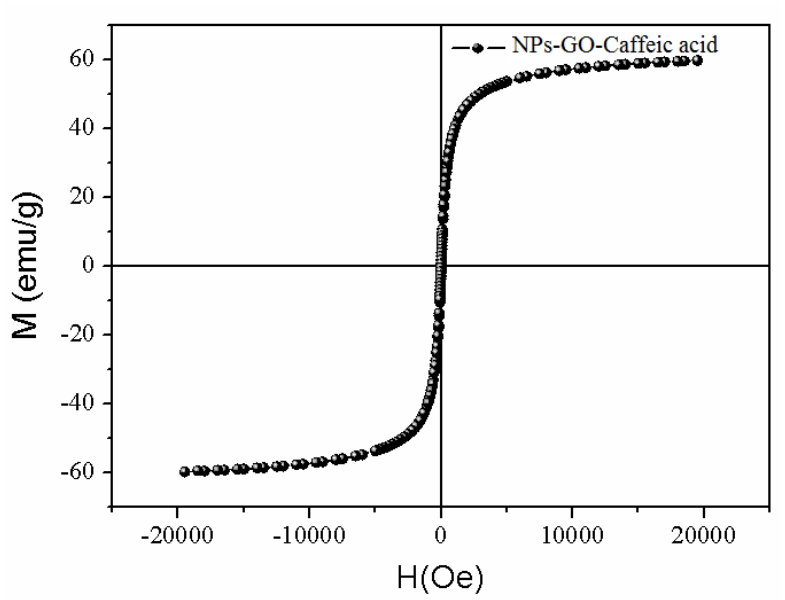
NPs-GO-Caffeic acid
M (emu/g)
H(Oe)
60
40
20
0
-20
-40
-60
-20000
-10000
0
10000
20000

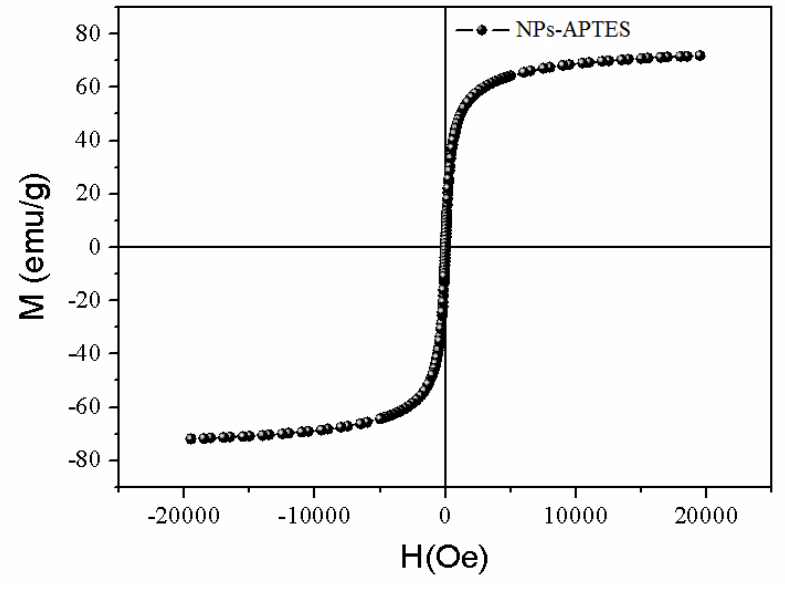
NPs-APTES
M (emu/g)
H(Oe)
80
60
40
20
0
-20
-40
-60
-80
-20000
-10000
0
10000
20000

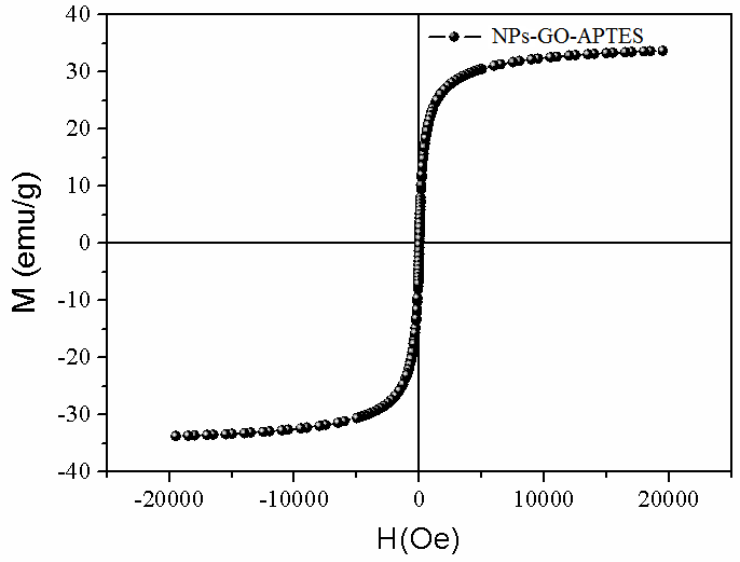

Figure 11.1: Magnetization curves of the different types of nanoparticles.

As shown in Table 11.1 and Figure 11.2, the saturation magnetization (M_s) of bulk magnetite and maghemite is higher than those of the nanoparticles, which means that the nanoparticles are less magnetic than the bulk material, as explained above.

Table 11.1: Saturation magnetization of bulk magnetite and maghemite and of the different types of nanoparticles.

Material	**M_s (emu/g)**
Bulk magnetite	100
Bulk maghemite	80
NPs	71
NPs-DHCA	68
NPs-CA	52
NPs-APTES	72
NPs-GO	35
NPs-GO-DHCA	23
NPs-GO-CA	60
NPs-GO-APTES	34

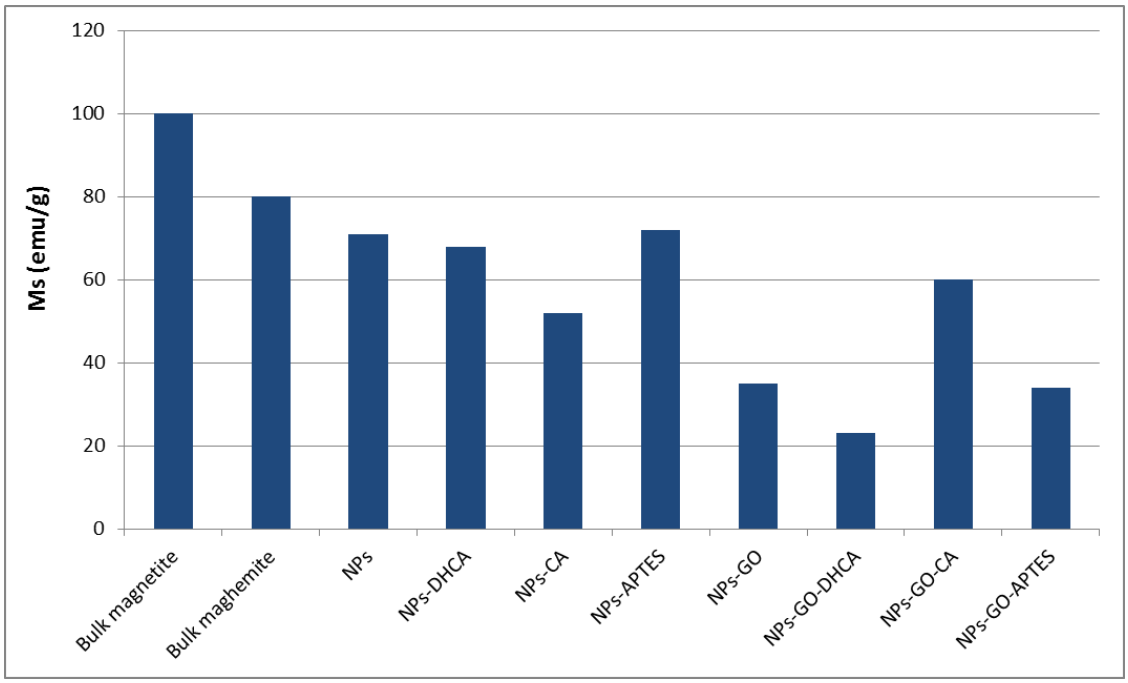

Figure 11.2: Comparison between the saturation magnetization of different types of bulk materials and nanoparticles.

Assuming an average saturation magnetization of 90 emu/g for a mixture of bulk maghemite and magnetite, it is possible to compare the saturation value of bulk and nanoscale material. In Table 11.2, it is shown that $NP_{S,}$ NPs-DHCA and NPs-APTES have a saturation equal to about 80% of bulk material saturation. Therefore DHCA and APTES do not significantly affect particles' magnetization.

NPs-Caffeic acid and NPs-GO-Caffeic acid saturation is about 60% of the bulk equivalent. All the values previously discussed are equal to or higher than values obtained by Kucheryavy at al. [31].

Instead, NPs-GO-DHCA and NPs-GO-APTES have only 30% of the saturation magnetization of the bulk equivalent.

Table 11.2: Saturation magnetization ratios of nanoscale and bulk material.

Nanoparticles	$\frac{M_{s,\,nanoparticles}}{M_{s,\,bulk\ material}}$
NPs	0,79
NPs-DHCA	0,76
NPs-CA	0,58
NPs-APTES	0,80
NPs-GO	0,39
NPs-GO-DHCA	0,26
NPs-GO-CA	0,67
NPs-GO-APTES	0,38

In the following table (Table 11.3) and graph (Figure 11.3) the saturation magnetizations of the nanocomposites with and without graphene oxide are compared. Generally GO addition leads to a relevant decrease of Ms, with the exception of nanoparticles functionalized with caffeic acid.

Table 11.3: Saturation magnetization ratios.

	M_s ratio
$\frac{M_{s,\,NPs-GO}}{M_{s,\,NPs}}$	0,49
$\frac{M_{s,\,NPs-GO-DHCA}}{M_{s,\,NPs-DHCA}}$	0,34
$\frac{M_{s,\,NPs-GO-CA}}{M_{s,\,NPs-CA}}$	1,15
$\frac{M_{s,\,NPs-GO-APTES}}{M_{s,\,NPs-APTES}}$	0,47

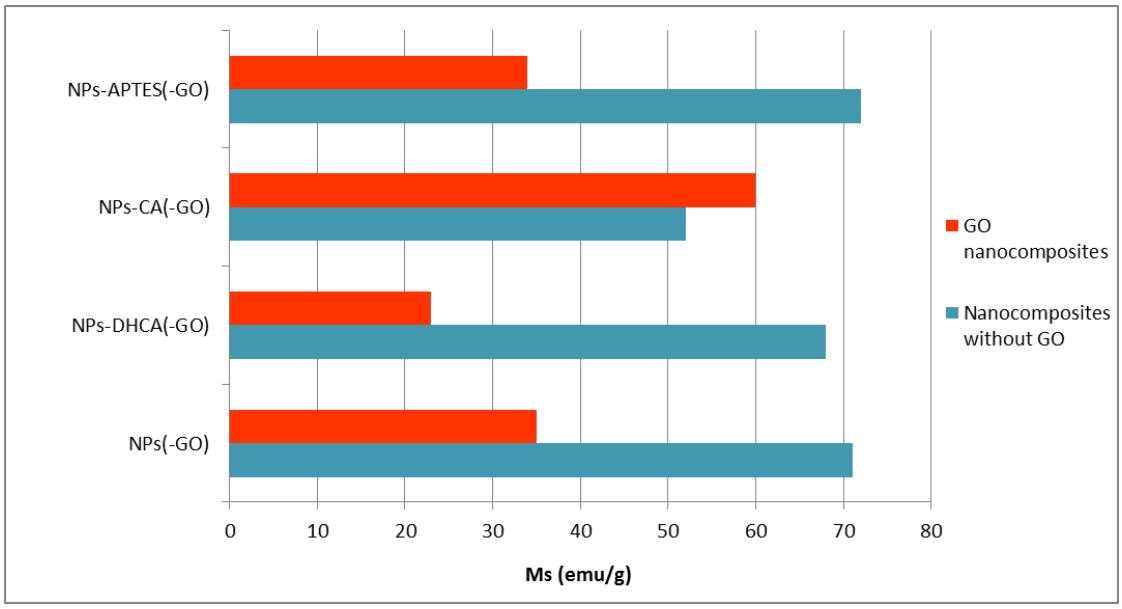

Figure 11.3: Comparison between the saturation magnetizations of the nanocomposites with and without graphene oxide.

12. Metals removal experiments

The amount of nanoparticles recovered by magnetic separation was weighted (Table 12.1, Table 12.2, Table 12.3). In almost all cases the amount of nanoparticles removed by magnetic separation was higher than 90% and often equal to 100%. This means that magnets are a good tool to remove NPs form water and they allow to avoid fouling problems that would occur if nanocomposites had to be collected by membrane filtration.

Table 12.1: Percentage of nanoparticles recovered by magnetic separation after lead removal.

Nanoparticles used	% NPs recovered by magnet
NPs	100
NPs-DHCA	90
NPs-CA	91,5
NPs-APTES	96,5
NPs-GO	100
NPs-GO-DHCA	100
NPs-GO-CA	99
NPs-GO-APTES	100

Table 12.2: Percentage of nanoparticles recovered by magnetic separation after chromium removal.

Nanoparticles used	% NPs recovered by magnet
NPs	65,5
NPs-DHCA	95,5
NPs-CA	100
NPs-APTES	60,5
NPs-GO	100
NPs-GO-DHCA	100
NPs-GO-CA	100
NPs-GO-APTES	100

Table 12.3: Percentage of nanoparticles recovered by magnetic separation after nickel removal.

Nanoparticles used	**% NPs recovered by magnet**
NPs	100
NPs-DHCA	94,5
NPs-CA	94
NPs-APTES	86
NPs-GO	100
NPs-GO-DHCA	100
NPs-GO-CA	100
NPs-GO-APTES	100

The remaining concentration of heavy metals after the adsorption experiments was measured with ICP-OES. Results obtained by the ICP are presented in Table 12.4, while Table 12.5 shows the same results corrected considering the dilution factor used before analyzing the sample, therefore presents the actual concentrations used during the experiments.

Table 12.4: Final concentrations of heavy metals after adsorption.

	Pb (µg/l)	**Cr** (µg/l)	**Ni** (µg/l)
Control sample	955	1100	1325
NPs	35,9	774	1245
NPs-DHCA	84	134	521
NPs-CA	55,2	169	384
NPs-APTES	74,1	371	789
NPs-GO	145	516	715
NPs-GO-DHCA	10	307	446
NPs-GO-CA	17,4	426	1040
NPs-GO-APTES	77	455	955

The initial concentration of heavy metals (concentrations in the control sample) are well above the Italian limit for discharge in surface water (0,2 mg/l for lead, 2 mg/l for nickel and total chromium). All nanocomposites managed to reduce lead below the legal

threshold. Only NPs-DHCA and NPs-Caffeic acid managed to obtain the same result in the case of chromium.

Table 12.5: Actual concentrations obtained at the end of experiment.

	Pb (mg/l)	**Cr** (mg/l)	**Ni** (mg/l)
Control sample	6,37	7,33	8,83
NPs	0,24	5,16	8,30
NPs-DHCA	0,56	0,89	3,47
NPs-CA	0,37	1,13	2,56
NPs-APTES	0,49	2,47	5,26
NPs-GO	0,97	3,44	4,77
NPs-GO-DHCA	0,07	2,05	2,97
NPs-GO-CA	0,12	2,84	6,93
NPs-GO-APTES	0,51	3,03	6,37

Table 12.6 and Figure 12.1 and show the amount of heavy metal removed in each experiment.

Table 12.6: Amount of heavy metal removed in each adsorption experiment.

	Pb (%)	**Cr** (%)	**Ni** (%)
NPs	96,24	29,64	6,04
NPs-DHCA	91,20	87,82	60,68
NPs-CA	94,22	84,64	71,02
NPs-APTES	92,24	66,27	40,45
NPs-GO	84,82	53,09	46,04
NPs-GO-DHCA	98,95	72,09	66,34
NPs-GO-CA	98,18	61,27	21,51
NPs-GO-APTES	91,94	58,64	27,92

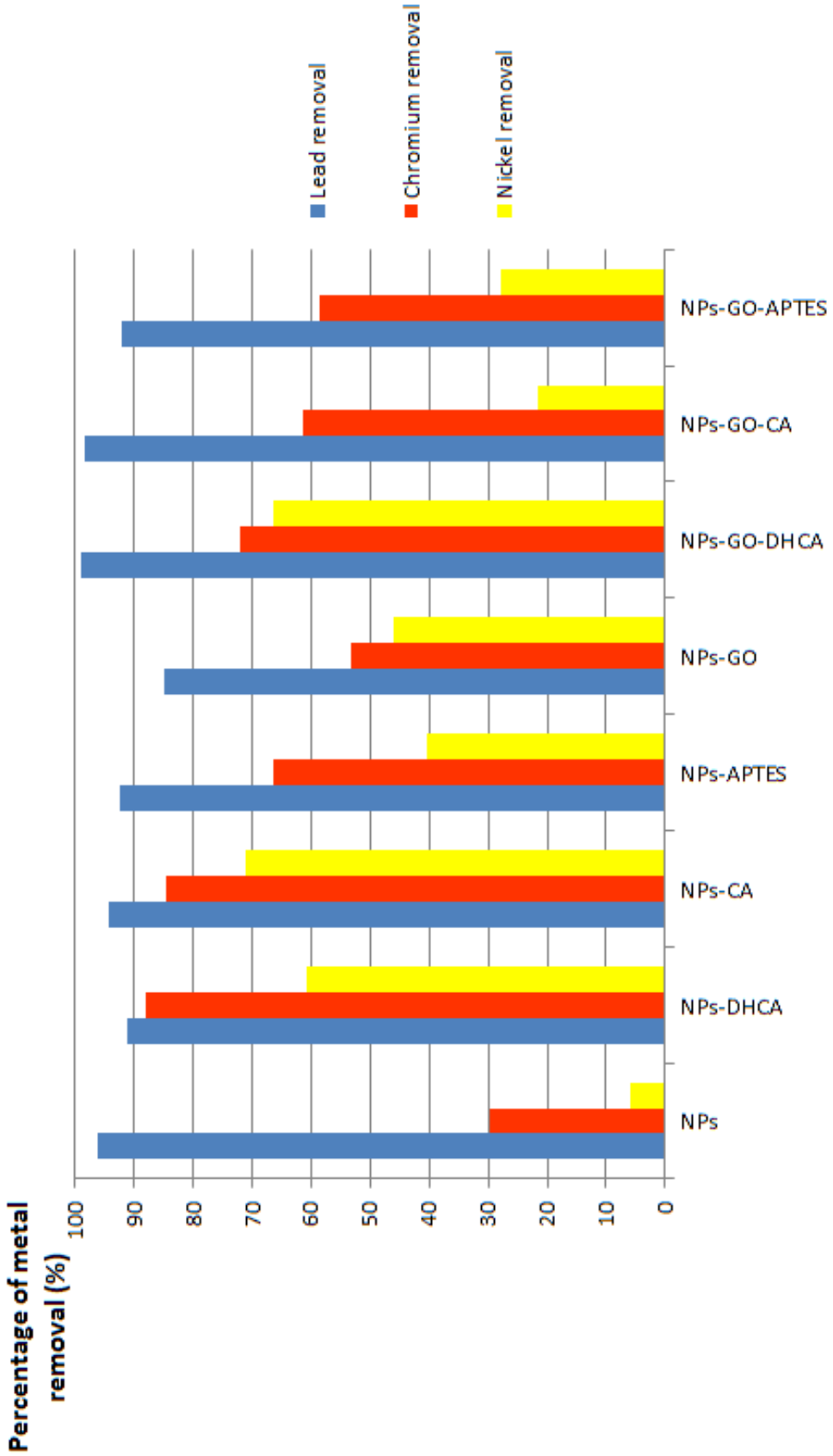

Figure 12.1: Amount of heavy metals removed by each type of nanocomposite.

Considering the similar initial concentration of the different metals, the removal percentages are comparable. The highest metal removal occurred for lead, while the lowest for nickel. Bare nanoparticles showed a very different behavior when treating different metals. Specifically, their performance dropped drastically from removing 96% of lead to removing just 6% of nickel. The performance does not change so drastically in the case of the other nanocomposites. This suggests that lead is probably removed by reduction and adsorption on the bare iron oxide nanoparticle surface, while the other metals are preferentially removed by coordination on the functionalized surface of the nanocomposite.

All nanoparticles worked well for lead removal. With the exception of NPs-GO nanoparticles (84% lead removal), they removed more than 90% of lead. NPs-GO-DHCA and NPs-GO-Caffeic acid almost completely removed the amount of lead present, removing more than 98% of the heavy metal. As shown in the following graph (Figure 12.2) GO addition improves significantly lead removal efficiency in nanoparticles functionalized with DHCA and caffeic acid.

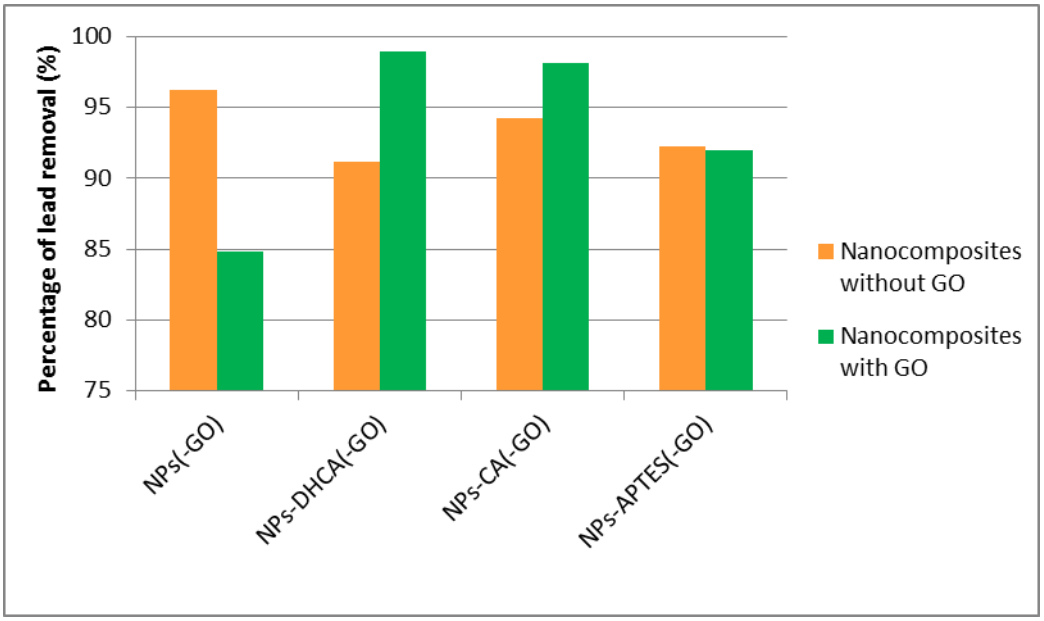

Figure 12.2: Comparison between the lead removal efficiency of nanocomposites with and without GO.

In the case of chromium, the nanoparticles with the highest efficiency are NPs-DHCA and NPs-Caffeic acid, removing more than 80% of the metal. Good removal percentages were obtained also with NPs-APTES, NPs-GO-DHCA and NPs-GO-Caffeic acid, which removed at least 60% of chromium. GO addition to the nanocomposites did not improve chromium removal as shown in Figure 12.3.

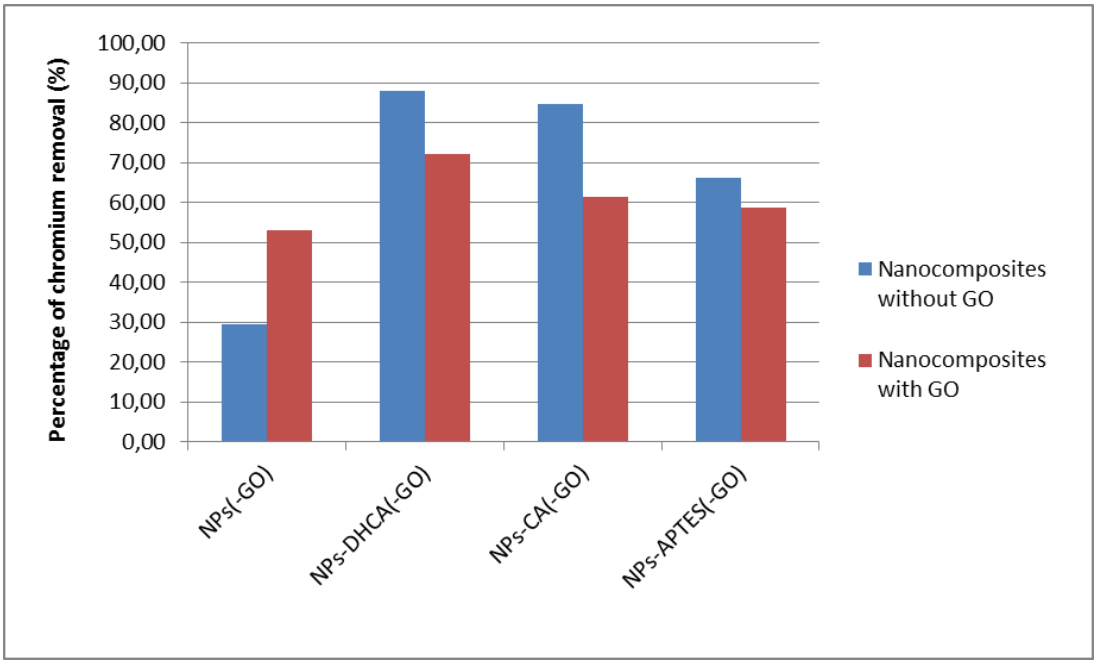

Figure 12.3: Comparison between the chromium removal efficiency of nanocomposites with and without GO.

Nanocomposites that removed more than 60% of nickel are NPs-DHCA, NPs-Caffeic acid and NPs-GO-DHCA, which showed good adsorption properties for all the three metals analyzed. Only in the case of nanoparticles functionalized with DHCA, GO addition to nanocomposites increases (5%) the nickel removal efficiency

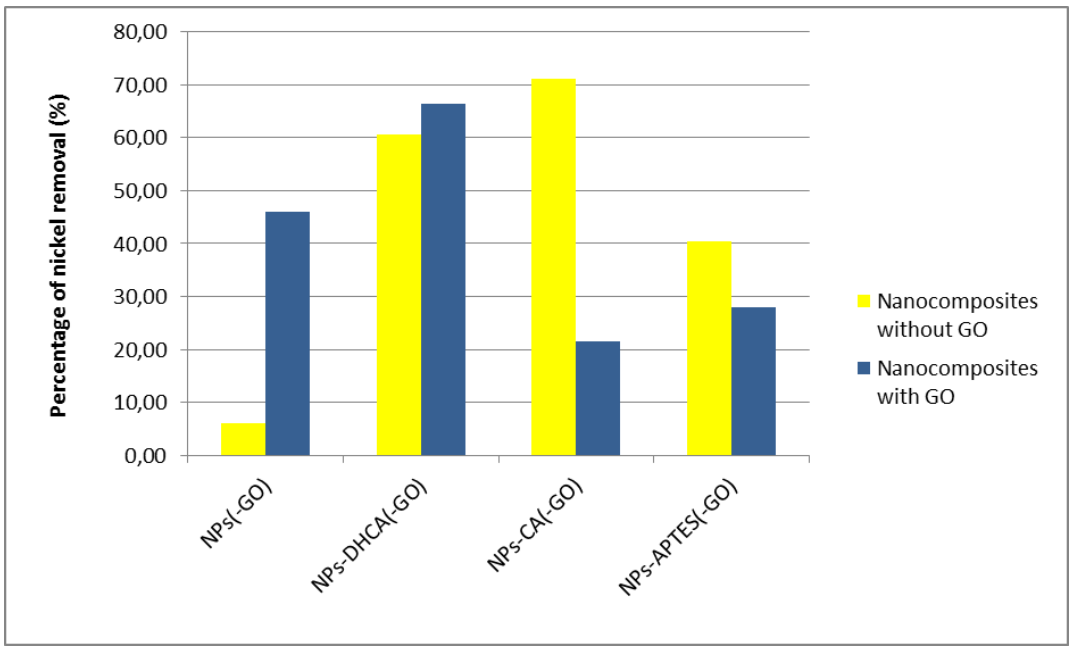

Figure 12.4: Comparison between the chromium removal efficiency of nanocomposites with and without GO.

Similar results can be find in literature even if adsorption experiment conditions and nanocomposites used often vary in different studies. For example, Liu et al. [32] using bare iron oxide nanoparticles, managed to remove 90% of lead.

As previously explained Mahdavian et al. [21] synthetized iron oxide nanoparticles functionalized with APTES and acryloyl chloride (AC) and converted to the corresponding sodium salt with an aqueous solution of NaOH. In order to compare the results obtained in the present study with those of Mahdavian et al., the adsorption of heavy metals was calculated, as shown in Table 12.7.

Table 12.7: Adsorption of heavy metals cations.

	Ads (mg_{Pb2+}/g_{NPs})	**Ads (mg_{Cr2+}/g_{NPs})**	**Ads (mg_{Ni2+}/g_{NPs})**
NPs	6,13	2,17	0,53
NPs-DHCA	5,81	6,44	5,36
NPs-CA	6,00	6,21	6,27
NPs-APTES	5,87	4,86	3,57
NPs-GO	5,40	3,89	4,07
NPs-GO-DHCA	6,30	5,29	5,86
NPs-GO-CA	6,25	4,49	1,90
NPs-GO-APTES	5,85	4,30	2,47

The results can be compared reminding that adsorption experiment conditions were different in the two cases. Nanocomposites synthetized by Mahdavian et al. showed higher adsorption capacity for lead and lower for nickel, as observed in the present study. However, adsorption capacity in the study of Mahdavian et al. was significantly higher (about 25 mg_{Ni2+}/g_{NPs}, and 30 mg_{Pb2+}/g_{NPs} at pH 7).

Ozmen et al. [22] analyzed copper removal with magnetite nanoparticles functionalized with APTES and glutaraldehyde (GA). With conditions similar to the present study applied during the adsorption experiments, they obtained the removal of 80% of the heavy metal.

13. Spreading and ecotoxicology of nanotechnologies

As shown in chapter 12, after wastewater treatment nanoparticles can be almost completely recovered by magnetic separation, therefore their release in the environment would be very limited. In any case, since nanotechnologies will be probably widely applied in the future, it is important to study their possible effects on the environment. New projects implementing nanoparticles are constantly developed, as shown for the United States in Figure 13.1. The map shows the locations of universities, companies and government laboratories that are using nanotechnologies in the US. The next figure (Figure 13.2) shows only those localized in the city of Los Angeles. According to the Project on Emerging Nanotechnologies these institutions are already 1200 only in the US. There are many nanotechnologies applied in the health and environmental fields (Figure 13.2, Figure 13.3), that are promising and allow to achieve targets impossible to obtain without them. However, with the increasing use of nanoparticles, also concerns about their environmental impact and their possible harmful effects on health are constantly growing.

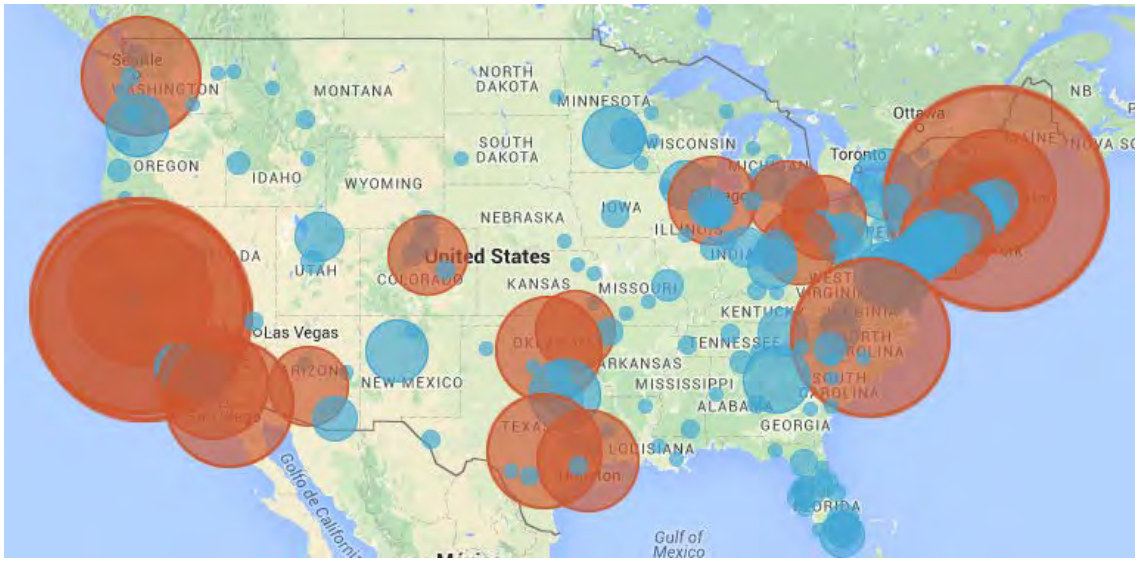

Figure 13.1: Map showing the localizations of companies and laboratories implementing nanotechnology in the US [33].

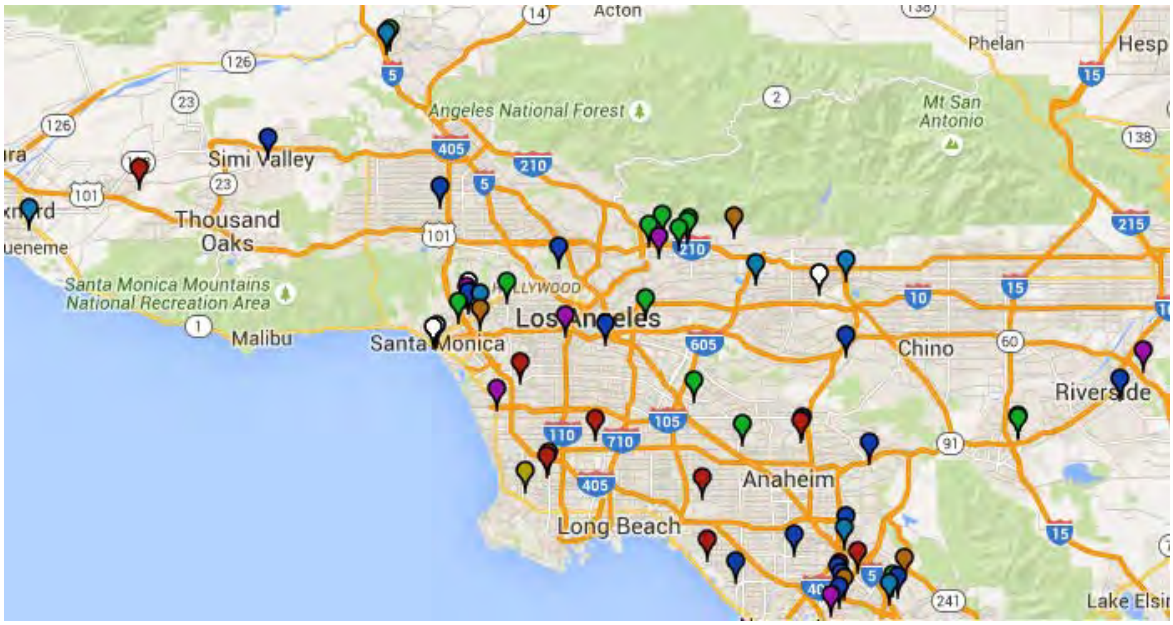

Figure 13.2: Map showing the localizations of companies and laboratories using nanotechnologies in the city of Los Angeles [33]. The different colors represent the different sectors in which the laboratory or company is working: orange, electronics; light blue, energy and environmental applications; yellow, imaging and microscopy; green, medicine and health; dark blue, materials; red, tools and instruments; purple, academic and government research; white, organization.

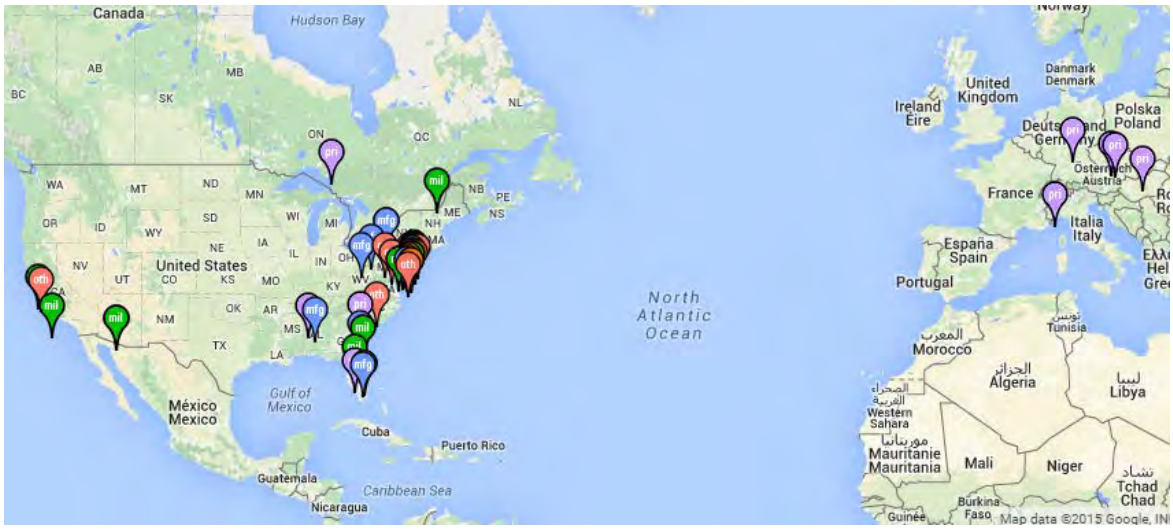

Figure 13.3: Map of contaminated sites where nanotechnologies are used worldwide [34].

Many of the properties that make nanotechnologies and nanoparticles useful, for example their high reactivity, may increase their potential risks towards human health and the environment. These risks are nowadays often still unknown and there is a need for further studies about the ecotoxicity of nanoparticles and nanocomposites.

All studies agree that different nanoparticles are characterized by different risks so case by case studies are needed. According to Handy et al. [35], manufactured nanoparticles

may behave differently with respect to naturally existing nanoparticles because designed to have specific properties. Furthermore nanoparticles that are not toxic may become harmful when carrying dangerous substances [36]. For example, Fe nanomaterials may bind with copper, which toxicity threshold for phytoplankton, algae fungi and flowering plants is exceeded only by mercury and sometimes silver [37].

13.1 Ecotoxicology of iron oxide nanoparticles

As stated in the previous paragraph, risk related to nanoparticles varies a lot with the type of particles considered. Concerns with respect to iron oxide nanoparticles are very low. As a matter of fact iron is a micronutrient, a substance essential for grow and survival in low amounts [38]. However, it is harmful at high concentrations. In particular, a study showed that iron oxide nanoparticles may cause considerable harmful effects on living organisms. Zhu et al. [39] used early life stages of the zebrafish (Danio rerio) in their study, since organisms in the early stages of embryonic development are usually more sensitive to toxicological effects. The concentration of iron oxide particles tested were 100, 50, 10, 5, 1, 0,5, 0,1 mg/l. According to this study, a concentration equal or higher to 10 mg/l of iron oxide nanoparticles caused developmental toxicity of Zebrafish embryos. The consequences of the exposure were mortality, hatching delay and malformations, as shown in the following graphs (Figure 13.4).

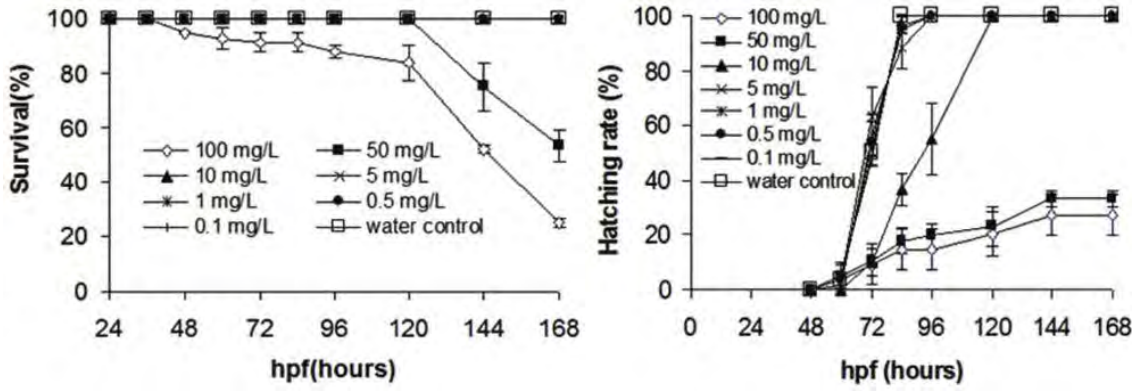

Figure 13.4: Different survival (on the left) and hatching rate (on the right) of zebrafish embryos caused by different concentration of iron oxide NPs over 168 hpf (hours postfertilization). Error bars represent the standard deviation from the mean of three replicates.

No effect on survival and no malformations were observed for nanoparticles concentrations ≤ 10 mg/l, however the hatching rate was influenced at a concentration of 10 mg/l.

Vittori Antisari et al, [40] found no effect on microbial biomass in soil with 10 and 100mg/kg of iron oxide NPs, which are the only metal oxide nanoparticles that show no or limited harmful effect on microbial communities even at high concentrations [41].

14. Conclusions

Stormwater volumes needing treatment will constantly increase in the foreseeable future. Heavy metals are one of the main categories of pollutants present in stormwater and have several adverse effect on human health. This thesis studies and compares new and previously synthetized nanocomposites for heavy metals removal from water. The synthesis and functionalization processes are easy to implement and the materials needed have limited costs.

Nanocomposites' magnetic properties allow to separate them magnetically from the water streams. Magnetic measurements and magnetic separation after adsorption experiments showed that these nanocomposites can efficiently be removed after their application simply by applying a magnet. These nanocomposites may therefore be implemented in a simple device where they would be injected in the wastewater stream, mixed and removed by magnetic means.

Heavy metals removal efficiency varies depending on the type of heavy metal (Pb > Cr > Ni). Removal was particularly efficient in the case of lead (Figure 14.1).

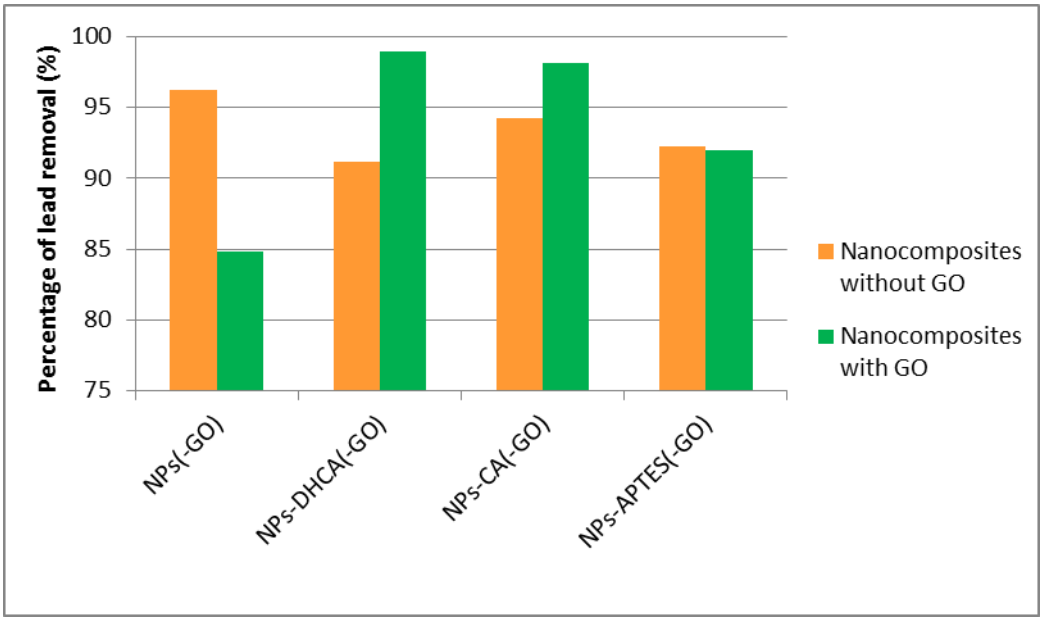

Figure 14.1: Removal efficiency of nanocomposites with and without GO.

Moreover the highest metal removal efficiency was reached by different nanocomposites depending on the metal considered:

- NPs-GO-DHCA and NPs-GO-Caffeic acid removed more than 98% of lead.
- NPs-DHCA and NPs-Caffeic acid removed more than 80% of chromium.
- NPs-DHCA, NPs-Caffeic acid and NPs-GO-DHCA removed more than 60% of nickel.

After application nanocomposites can be recycled by using chemicals to remove the heavy metals captured. Obviously, this would increase the amount of chemicals used in the process. Considering the low costs of the nanocomposites implemented, an alternative would be to discard the metals remaining after removal of graphene oxide by thermal treatment.

Further research must assess the behavior of nanocomposites when different heavy metals are present in water, in order to study the selectivity of the removal process. Moreover adsorption experiments should be carried out on metals different from the ones analyzed in this thesis and on substences different from heavy metals. Finally other functionalization may be studied to improve the removal efficiency.

15. Bibliography

[1] Rupak Aryal, Sarvanamuthu Vigneswaran,, Jaya Kandasamy, and Ravi Naidu, "*Urban stormwater quality and treatment*", Korean J. Chem. Eng. 2010, 27, 1343.

[2] M.A. Barakat, "*New trends in removing heavy metals from industrial wastewater*", Arabian Journal of Chemistry 2011, 4, 361.

[3] Allen P. Davis, Mohammad Shokouhian and Shubei Ni, "*Loading estimates of lead, copper, cadmium and zinc in urban runoff from specific sources*", Chemosphere 2001, 44, 997.

[4] http://archivio.ambiente.it/impresa/legislazione/leggi/1999/dlgs152-99/allegato5.htm.

[5] Regolamento Regionale 24 marzo 2006 , N. 4. Disciplina dello smaltimento delle acque di prima pioggia e di lavaggio delle aree esterne, in attuazione dell'articolo 52, comma 1, lettera a) della legge regionale 12 dicembre 2003, n. 26.

[6] http://www.eurowater.com/products/standard_products/nanofiltration_plants.aspx.

[7] Chen, G.H.,. "*Electrochemicals technologies in wastewater treatment"*, Separation and Purification Technologies 2004, 38 (1), 11.

[8] Herrmann, J.M.,. "*Heterogeneous photocatalysis: fundamentals and applications to the removal of various types of aqueous pollutants*.", Catalysis Today 1999, 53, 115.

[9] N. Savage, Mamadou Diallo, Jeremiah Duncan, Anita Street and Richard Sustich, "*Nanotechnology Applications for Clean Water"*, William Andrew Ed., 2009.

[10] Iram Mohmood, Clàudia Batista Lopes, Isabel Lopes, Iqbal Ahmad, Armando C. Duarte, Eduarda Pereira, "*Nanoscale materials and their use in water contaminants removal (a review)*", Environmental Science Pollution Research 2013, 20, 1239.

[11] Bharat Bhushan, "*Springer Handbook of Nanotechnology - Introduction to Nanotechnology*", Ed. Springer, 2007.

[12] Wei-xian Zhang, "*Nanoscale iron particles for environmental remediation: An overvie*w" Journal of Nanoparticle Research 2003, 5 ,323.

[13] Paul G. Tratnyek, Richard L. Johnson, "*Nanotechnologies for environmental cleanup*" Nano Today 2006, 1, 44.

[14] Kimberly M. Cross, Yunfeng Lu, Tonghua Zheng, Jingjing Zhan, Gary McPherson, Vijay John, "*Water Decontamination Using Iron and Iron Oxide Nanoparticles*" Nanotechnology Applications for Clean Water 2009, 347.

[15] Samuel C.N. Tang, Irene M.C. Lo, "*Magnetic nanoparticles: Essential factors for sustainable environmental applications*", Water Research 2013, 47, 2613.

[16] Thomas M. McCoy, Paul Brown, Julian Eastoe, Rico F. Tabor, "*Noncovalent Magnetic Control and Reversible Recovery of Graphene Oxide Using Iron Oxide and Magnetic Surfactants*", Applied Materials & Interfaces 2014, 7, 2124.

[17] Abolfazl Akbarzadeh, Mohamad Samiei and Soodabeh Davaran, "*Magnetic nanoparticles: preparation, physical properties, and applications in biomedicine*", Nanoscale Research Letters 2012, 7:144.

[18] Hilda W. F. Sung and Czeslaw Rudowicz, "*A closer look at the hysteresis loop for ferromagnets*", Department of Physics and Materials Science, City University of Hong Kong.

[19] Sophie Laurent, Delphine Forge, Marc Port, Alain Roch, Caroline Robic, Luce Vander Elst, Robert N. Muller, "Magnetic Iron Oxide Nanoparticles: Synthesis, Stabilization, Vectorization, Physicochemical Chacterization and Biological Applications", Chemical Reviews 2008, 108, 2064.

[20] Borsella Elisabetta, D'Amato Rosaria, Fabbri Fabio, Falconieri Mauro, Terranova Gaetano, "*Synthesis of nanoparticles by laser pyrolysis: from research to applications"*, Energia, Ambiente e Innovazione 2011, 4-5, 54.

[21] Ali Reza Mahdavian, Monir Al-Sadat Mirrahimi, "*Efficient separation of heavy metal cations by anchoring polyacrylic acid on superparamagnetic magnetite nanoparticles through surface modification*", Chemical Engineering Journal 2010, 159, 264.

[22] Mustafa Ozmen, Keziban Can, Gulsin Arslan, Ali Tor, Yunus Cengeloglu, Mustafa Ersoz, "*Adsorption of Cu(II) from aqueous solution by using modified Fe3O4 magnetic nanoparticles*", Desalination 2010, 254, 162.

[23] Paul N. Diagboya, Bamidele I., Olu-Owolabi and Kayode O. Adebowale, "*Synthesis of covalently bonded graphene oxide–iron magnetic nanoparticles and the kinetics of mercury removal*", Royal Society of Chemistry 2015, 5, 2536.

[24] Caterina Soldano, Ather Mahmood, Erik Dujardin, "*Production, properties and potential of graphene*", Carbon 2010 , 48, 2127.

[25] Da Chen, Hongbin Feng, Jinghong Li, "*Graphene Oxide: Preparation, Functionalization and Electrochemical Applications*", Chemical Reviews 2012, 112(11), 6027.

[26] Liu Y., Chen T., Wu C., Qiu L., Hu R., Li J., Cansiz S., Zhang L., Cui C., Zu G., You M., Zhang T., Tan W., "*Facile surface functionalization of hydrophobic magnetic nanoparticles"*, Journal of the American Society 2014, 136, 12552.

[27] Flavio Pendolino, Emilio Parisini, and Sergio Lo Russo, "*Time-Dependent Structure and Solubilization Kinetics of Graphene Oxide in Methanol and Water Dispersions*", The journal of Physical Chemistry 2014, 28, 162.

[28] George Z. Kyzas, Eleni A. Deliyanni, Kostas A. Matis, "*Graphene oxide and its application as an adsorbent in wastewater treatment*", Journal of Chemical Technology and Biotechnology 2014, 89, 196.

[29] Laureti Sara, tesi di dottorato di ricerca in Scienza dei Materiali (Roma, Università La Sapienza 23/12/2007).

[30] MIT OpenCourseWare, "*Geochemical Analysis of Environmental Materials"*, Analytical Techniques for Studying Environmental and Geologic Samples, Spring 2011.

[31] Pavel Kucheryavy, Jibao He, Vijay T. John, Pawan Maharjan, Leonard Spinu, Galina Z.Goloverda, and Vladimir L. Kolesnichenko, "*Superparamagnetic Iron Oxide Nanoparticles with Variable Size and an Iron Oxidation State as Prospective Imaging Agents*", American Chemical Society 2012, 29(2), 710.

[32] Jing-Fu Liu, Zong-Shan Zhao and Gui-Bin Jiang, *"Coating of Fe_3O_4 Magnetic Nanoparticles with Humic Acid for High Efficient Removal for Heavy Metals in Water"*, Environ. Sci. Technol. 2008, 42, 6949.

[33] http://www.nanotechproject.org/inventories/map/.

[34] http://www.nanotechproject.org/inventories/remediation_map/.

[35] Handy RD, von der Kammer F., Lead JR, Hassellöv M., Owen R., Crane M., "*The ecotoxicology and chemistry of manufactured nanoparticles*", Ecotoxicology 2008, 17, 287.

[36] Barbara Karn, Todd Kuiken, Martha Otto, "*Nanotechnology and in Situ Remediation: A Review of the Benefits and Potential Risks*", Environmental Health Perspectives 2009, 117, 1823.

[37] Sposito G., *"The Chemistry of Soils"*, Ed. University Press, 1989.

[38] Verónica Nogueira, Isabel Lopes, Teresa Rocha-Santos, Fernando Goncalves, Ruth Pereira, "*Toxicity of solid residues resulting from wastewater treatment with nanomaterials*, Aquatic Toxicology 2015, 165, 172–178.

[39] Xiaoshan Zhu, Shengyan Tian, Zhonghua Cai "*Toxicity Assessment of Iron Oxide Nanoparticles in Zebrafish (Danio rerio) Early Life Stages"*, PLoS ONE 2012, 7(9), 1.

[40] Vittori Antisari L, Carbone S, Gatti A, Vianello G, Nannipieri P., "*Toxicity of metal oxide (CeO2, Fe3O4, SnO2) engineered nanoparticles on soil microbial biomass and their distribution in soil."*, Soil Biology and Biochemistry 2015, 60, 87‑94.

[41] Marie Simonin, Agnès Richaume, "*Impact of engineered nanoparticles on the activity, abundance, and diversity of soil microbial communities: a review"*, Environmental Science and Pollution Research 2015.